

## PAIN

# Green light analgesia in mice is mediated by visual activation of enkephalinergic neurons in the ventrolateral geniculate nucleus

Yu-Long Tang, Ai-Lin Liu, Su-Su Lv, Zi-Rui Zhou, Hong Cao\*, Shi-Jun Weng\*, Yu-Qiu Zhang\*

Copyright © 2022  
The Authors, some  
rights reserved;  
exclusive licensee  
American Association  
for the Advancement  
of Science. No claim  
to original U.S.  
Government Works

Green light exposure has been shown to reduce pain in animal models. Here, we report a vision-associated enkephalinergic neural circuit responsible for green light-mediated analgesia. Full-field green light exposure at an intensity of 10 lux produced analgesic effects in healthy mice and in a model of arthrosis. Ablation of cone photoreceptors completely inhibited the analgesic effect, whereas rod ablation only partially reduced pain relief. The analgesic effect was not modulated by the ablation of intrinsically photosensitive retinal ganglion cells (ipRGCs), which are atypical photoreceptors that control various nonvisual effects of light. Inhibition of the retino-ventrolateral geniculate nucleus (vLGN) pathway completely abolished the analgesic effects. Activation of this pathway reduced nociceptive behavioral responses; such activation was blocked by the inhibition of pro-enkephalin (Penk)-positive neurons in the vLGN (vLGN<sup>Penk</sup>). Moreover, green light analgesia was prevented by knockdown of *Penk* in the vLGN or by ablation of vLGN<sup>Penk</sup> neurons. In addition, activation of the projections from vLGN<sup>Penk</sup> neurons to the dorsal raphe nucleus (DRN) was sufficient to suppress nociceptive behaviors, whereas its inhibition abolished the green light analgesia. Our findings indicate that cone-dominated retinal inputs mediated green light analgesia through the vLGN<sup>Penk</sup>-DRN pathway and suggest that this signaling pathway could be exploited for reducing pain.

## INTRODUCTION

The high prevalence of chronic pain is a global public health priority (1); there is a need for the development of effective approaches without side effects. Light therapy holds potential as a noninvasive, convenient, and cost-effective option. Exposure to light of specific wavelengths and intensities has shown some effects in the management of various health conditions, such as cancers (2), skin diseases (3), sleep disorders (4), and affective disorders (5). Recently, low-intensity laser/light therapy has been used for the management of various pain conditions, including chronic nonspecific low back pain (6), fibromyalgia pain (7), migraine headaches (8), and neuropathic pain (9). Among the colors and wavelengths available for such therapy, most studies have reported the beneficial effects of green light (10). Clinical and preclinical studies demonstrated that green light-emitting diodes (LEDs) were particularly efficacious for pain relief in rats after nerve injury and in patients with migraine or fibromyoma (8, 11–13). The use of opaque contact lenses completely eliminated the analgesic effect of green LED exposure in rats (11), implying that the visual system contributes to those effects. However, the ocular photoreceptor(s) and visual circuits underlying green light analgesia remain largely unknown.

The mammalian eye contains three classes of photoreceptors with distinct peak excitation wavelength and photoresponse characteristics: rod and cone ("canonical" photoreceptors) in the outer retina (14) and melanopsin-expressing intrinsically photosensitive retinal ganglion cell (ipRGC; "noncanonical" photoreceptor) in the inner retina (15). Both rod/cone photoreceptors and ipRGCs may participate in photobiomodulation. For example, ipRGC/

melanopsin-mediated photo signals are reportedly involved in mood and learning/memory regulation (16–19), along with bright light-induced antinociception (20, 21), whereas cone- and rod-driven retinal pathways are involved in migraine photophobia (22, 23). Elucidation of the exact photoreceptor class responsible for light-induced analgesia could allow the development of more efficient pain-management strategies.

The lateral geniculate nucleus (LGN) is a core retinorecipient brain region; it includes a dorsal part (dLGN) and a ventral part (vLGN). Generally, the dLGN is responsible for image-forming (pattern) vision; the vLGN, which is innervated by both conventional RGCs (cRGCs) and ipRGCs, contributes to various non-image-forming visual functions (24, 25). The retino-vLGN circuit has been shown to participate in the therapeutic effects of light on both depressive and nocifensive symptoms (19, 20). Although mostly GABAergic, neurons in the vLGN exhibit robust neuromodulator heterogeneity (26). Specifically, a subset of these neurons expresses enkephalin (ENK), an endogenous opioid peptide that is implicated in pain control (27, 28). Here, we identified a visual circuit in mice that conveys light signals (primarily from cone photoreceptors) to ENK-positive neurons in the vLGN and subsequently to the dorsal raphe nucleus (DRN). We aimed to study whether this pathway mediates green light-induced analgesia.

## RESULTS

### Cones and rods contributed to the analgesic effects of green light in mice

Repeated low-intensity green light (525 nm, 4 to 110 lux) exposure has been shown to produce long-lasting antinociceptive effects in rats; this effect can be blocked by dark opaque lenses, suggesting a role for the visual system in green light analgesia (11). To determine the mechanism mediating green light analgesia, we first investigated

State Key Laboratory of Medical Neurobiology and MOE Frontiers Center for Brain Science, Institutes of Brain Science, Fudan University, Shanghai 200032, China.

\*Corresponding author. Email: yuqiuzhang@fudan.edu.cn (Y.-Q.Z.); hongcao@fudan.edu.cn (H.C.); sjweng@fudan.edu.cn (S.-J.W.)

which classes of retinal photoreceptors could be involved in the analgesic effects using a mouse model of arthritic pain.

Unilateral intra-articular injection of complete Freund's adjuvant (CFA) produced marked joint inflammation (edema and erythema), thermal hyperalgesia, and mechanical allodynia in ipsilateral hind paw (fig. S1, A to C). Arthritic mice exposed to green light (523 nm, 10 lux,  $5.07 \times 10^9$  quanta/cm<sup>2</sup>·s, full-body exposure) for 8 hours daily during the light cycle (8:00 a.m. to 4:00 p.m.) for six consecutive days exhibited significant relief from CFA-induced thermal hyperalgesia and mechanical allodynia [Fig. 1, A to C, two-way repeated measures (RM) analysis of variance (ANOVA); paw withdrawal latencies (PWLs):  $F_{1,18} = 86.8$ ,  $P < 0.0001$ ; paw withdrawal thresholds (PWTs):  $F_{1,18} = 49.7$ ,  $P < 0.0001$ ]. In naive and sham mice, green light exposure suppressed nociceptive responses to noxious heat stimulation but did not affect von Frey tactile stimulation (fig. S2, A to D). We also examined the effects of green light exposure for 5 hours daily during the light cycle (8:00 a.m. to 1:00 p.m.) and 8 hours daily during the dark cycle (12:00 a.m. to 8:00 a.m.) for six consecutive days. Mechanical allodynia was reversed in the CFA-arthritic mice, whereas thermal hyperalgesia was not (fig. S3, A to D). These results indicate that the green light analgesic effect was modulated by dose and time of exposure. For the subsequent experiments, light exposure was applied at 8:00 a.m. to 4:00 p.m., the most effective protocol.

To determine whether retinal rod and cone photoreceptors mediated the green light analgesia, *N*-methyl-*N*-nitrosourea (MNU), a direct-acting alkylating agent that induces specific photoreceptor degeneration (29), was injected intraperitoneally (i.p., 65 mg/kg). After MNU injection, peanut agglutinin lectin (cone marker)– and rhodopsin (rod marker)–positive signals were largely absent in the outer retina, and the outer nuclear layer was thinned, whereas neurons in the ganglion cell layer and inner nuclear layer, including bipolar cells that are closely adjacent to photoreceptors, were not affected (Fig. 1D and fig. S4A). In addition, no obvious neuron damage was found in central visual areas such as the primary visual cortex (V1) and vLGN (fig. S4B). The analgesic effects of green light were completely eliminated in CFA-arthritic mice (two-way RM ANOVA; PWLs:  $F_{1,14} = 42.2$ ,  $P < 0.0001$ ; PWTs:  $F_{1,14} = 30.5$ ,  $P < 0.0001$ ; Fig. 1, E to G). This finding suggested that rods and/or cones may contribute to green light analgesia. To evaluate the roles of rod and cone photoreceptors in green light analgesia separately, we used cone–diphtheria toxin A (DTA) mice, in which cone photoreceptors were genetically ablated using a cone-specific DTA (30), and *Gnat1*<sup>−/−</sup> mice, which lack rod function because they do not have the gene encoding rhodopsin-associated G protein–transducing  $\alpha 1$  (31). Green light exposure failed to induce analgesic effects in cone-DTA mice, whereas it was partially effective in *Gnat1*<sup>−/−</sup> mice (two-way RM ANOVA; PWLs:  $F_{2,35} = 34.9$ ,  $P < 0.0001$ ; PWTs:  $F_{2,35} = 32.8$ ,  $P < 0.0001$ ; Fig. 1, H to K). These results indicate that retinal cones were required for green light analgesia, whereas rods, although also participating in this process, seemed to be only partially involved.

### Green light analgesia was independent of ipRGCs

ipRGCs comprise a class of atypical RGCs. They capture light using a G protein–coupled receptor known as melanopsin and are considered ganglion cell photoreceptors. In addition to their well-established role in non–imaging-forming visual functions (such as

photic regulation of circadian rhythms and pupillary light responses), recent studies have revealed their involvement in higher functions such as affective behavior, learning, and memory (18). To determine whether these cells participate in green light analgesia, melanopsin-SAP, an anti-melanopsin antibody-conjugated ribosome-inactivating protein saporin (SAP), was injected intravitreally bilaterally to selectively ablate ipRGCs (32). Melanopsin-SAP (400 ng) injection effectively reduced the density of ipRGCs (obtained by counting the number of melanopsin-immunoreactive somata) by >80%, without obvious damage to rod/cone photoreceptors or cRGCs (Fig. 2, A to D). Unlike the ablation of outer retinal rod and cone photoreceptors, ipRGC ablation did not affect green light analgesia (Fig. 2, E to G). Considering that melanopsin's excitation peak is in the blue (33), we also examined the effects of ipRGC ablation on blue light analgesia. It has been proved that blue light (472 nm, 110 lux,  $4 \times 10^{10}$  quanta/cm<sup>2</sup>·s) exposure for 8 hours daily for five consecutive days produced antinociceptive effects (11). Similar to green light, the analgesic effects of blue light were not affected by melanopsin-SAP injection (two-way RM ANOVA; PWLs:  $F_{3,25} = 4.6$ ,  $P = 0.01$ ; PWTs:  $F_{3,25} = 3.9$ ,  $P = 0.02$ , Fig. 2, F and G). In addition, the analgesic effects of green light were present in melanopsin knockout in *Opn4*<sup>−/−</sup> mice, implying that excitation of this unique photopigment is not required for the green light analgesia (Fig. 2, H to J). The above data imply that melanopsin and ipRGC are likely not involved in the green light analgesia in arthritic mice.

### Activation of retino-vLGN projection was required for green light analgesia

We next attempted to identify the retina-innervated central nuclei responsible for the green light analgesia. Anterograde tracing signals were observed bilaterally in the superior colliculus (SC) and LGN (including dLGN and vLGN) after intravitreal injection of fluorescently labeled cholera toxin subunit B (CTB; Fig. 3, A and B). Engineered G<sub>i/o</sub>-coupled human muscarinic M4 designer (hM4Di) receptor exclusively activated by designer drugs virus (Syn-hM4Di-mCherry) or Syn-mCherry (control) was injected bilaterally into the SC, dLGN, and vLGN. Chemogenetic inhibition of SC and dLGN neurons by intraperitoneal injection of clozapine-*N*-oxide (CNO) did not modify the analgesic effects of green light in CFA-arthritic mice (Fig. 3, C to K). In contrast, chemogenetic inhibition of the vLGN, another area receiving inputs from the retina involved in multiple non–image-forming visual functions (18, 19), had significant suppressive effects on green light analgesia (two-way RM ANOVA; PWLs:  $F_{2,17} = 5.9$ ,  $P = 0.01$ ; PWTs:  $F_{2,17} = 8.4$ ,  $P = 0.003$ ; Fig. 4, A to E). These findings imply that the vLGN, but not the dLGN and SC, is required for green light analgesia, although all three brain areas receive direct retinal inputs.

To verify the role of retino-vLGN projections in green light analgesia further, we injected adeno-associated virus 2/1–expressing Cre recombinase (AAV2/1-Cre) bilaterally into the vitreous cavity and a double-floxed inverted open-reading frame (DIO) construct encoding hM4Di (DIO-hM4Di-mCherry) virus bilaterally into the vLGN to infect vLGN postsynaptic neurons specifically with hM4Di or mCherry (Fig. 4, F and G). AAV2/1-Cre from transduced presynaptic neurons was able to effectively drive Cre-dependent transgene expression in selected postsynaptic neuronal targets (34). Thus, vLGN neurons receiving RGC axonal projections were selectively inhibited (Fig. 4, H and I). The results show that inhibition of

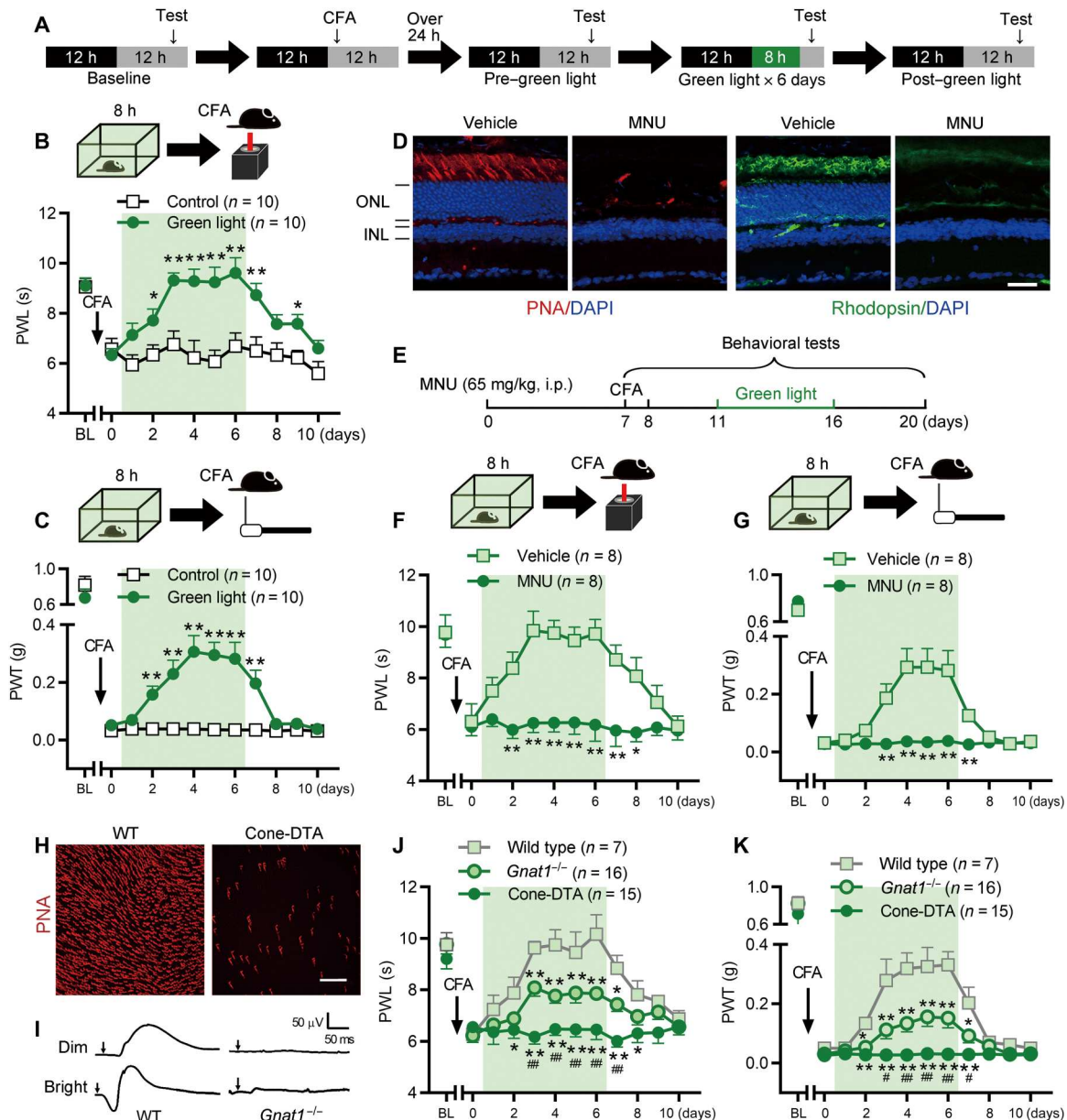


**Fig. 1. Retinal cones and rods were required for the analgesic effects of green light in CFA-arthritic mice.** (A) Schematic of the experimental design. (B and C) Effect of green light exposure on complete Freund's adjuvant (CFA)-induced thermal hyperalgesia (B) and mechanical allodynia (C). \* $P < 0.05$  and \*\* $P < 0.01$  versus control. (D) Retinal vertical sections showing peanut agglutinin lectin (PNA; cone marker)-positive and rhodopsin (rod marker)-positive signals after intraperitoneal administration of MNU. Scale bar, 30  $\mu\text{m}$ . (E) Schematic of the protocol in experiments (F) and (G). (F and G) Effect of green light after MNU treatment. \* $P < 0.05$  and \*\* $P < 0.01$  versus vehicle control. (H) Retinal whole mounts showing PNA-positive signals in the retinas of Cone-DTA mice. Scale bar, 100  $\mu\text{m}$ . (I) Dark-adapted ERGs recordings showing ERG responses to dim and bright flashes in *Gnat1*<sup>-/-</sup> mice. (J and K) Effect of green light in wild-type, Cone-DTA, and *Gnat1*<sup>-/-</sup> mice. \* $P < 0.05$  and \*\* $P < 0.01$  versus wild-type mice; # $P < 0.05$  and ## $P < 0.01$  versus *Gnat1*<sup>-/-</sup> mice. Two-way repeated measures (RM) ANOVA followed by post hoc Student-Newman-Keuls test (B, C, F, G, J, and K). Data are expressed as means  $\pm$  SEM. Sample sizes are indicated in parentheses. PWL, paw withdrawal latency; PWT, paw withdrawal threshold; BL, baseline; MNU, *N*-methyl-*N*-nitrosourea.

vLGN postsynaptic neurons receiving retinal projections efficiently blocked green light analgesia (Fig. 4, J and K, and fig. S5, A to E). These data indicate that the retino-vLGN projection mediates green light analgesia in rodents.

We also found that the analgesic effect of green light was absent in *Tra2b* conditional knockout mice with major cortex loss, including V1 loss (35, 36) (fig. S6). These results suggest that the cortical

structural integrity and functional integrity are required for green light analgesia.

### Activation of the retino-vLGN pathway produced analgesia in CFA-arthritic mice

We used optogenetic manipulation to investigate further whether activation of the retino-vLGN circuit directly produced analgesia.



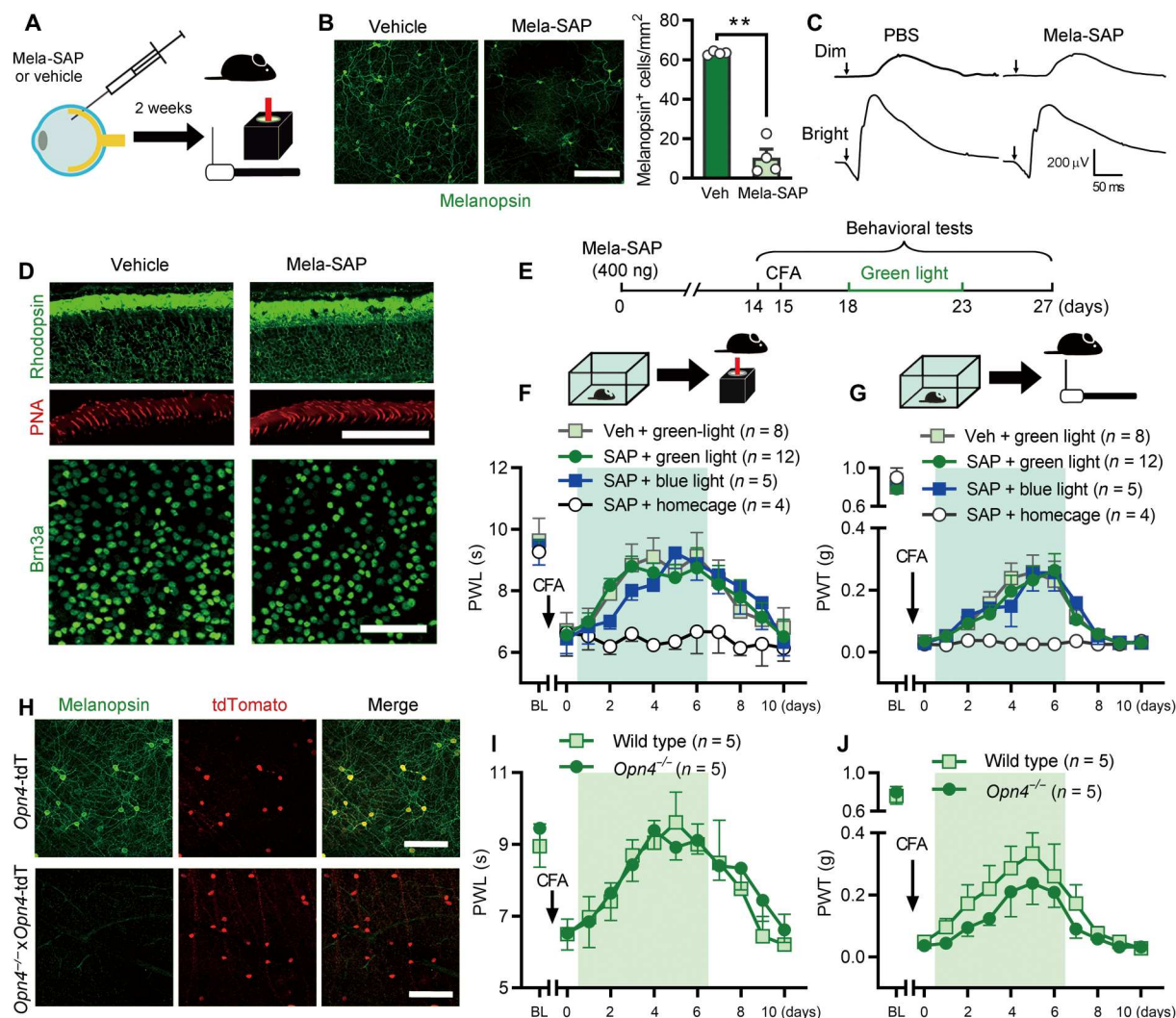


**Fig. 2. Retinal ipRGCs and melanopsin were not involved in green light analgesia in CFA-arthritic mice.** (A) Schematic of intravitreal injection of melanopsin-saporin (Mela-SAP; left) and von Frey and Hargreaves' tests (right). (B) Retinal whole mounts showing melanopsin (UF008 antibody)-positive cells after Mela-SAP injection. Scale bar, 200  $\mu$ m.  $^{**}P < 0.01$  (two-tailed Student's *t* test; *n* = 4). (C) Dark-adapted ERG recordings showing response to dim and bright flashes after Mela-SAP injection. Arrows indicate the 3-ms flashes. (D) Retinal vertical sections (top and middle) and whole mounts (bottom) showing rhodopsin-positive (rod marker, top), PNA-positive (cone marker, middle), and Brn3a-positive (cRGC marker, bottom) signals after Mela-SAP injection. Scale bars, 200  $\mu$ m. (E) Schematic of the protocol in experiments (F) and (G). (F and G) Effect of intravitreal injection of Mela-SAP on green and blue light analgesia. (H) Retinal whole mounts showing melanopsin-immunoreactive signals in the retinas from an *Opn4*<sup>-/-</sup> mouse and an *Opn4*-tdTomato (*Opn4*-tdT) mouse. Scale bars, 200  $\mu$ m. (I and J) Effect of green light exposure on CFA-induced thermal hyperalgesia (I) and mechanical allodynia (J) in *Opn4*<sup>-/-</sup> and wild-type mice. Two-way RM ANOVA (F, G, I, and J). Data are expressed as means  $\pm$  SEM. Sample sizes are indicated in parentheses.

An AAV-encoding channelrhodopsin-2 (ChR2) was injected bilaterally into the vitreous cavity in mice; optical fibers were placed into the vLGN (Fig. 5, A and B). Although a fraction of ipRGCs release  $\gamma$ -aminobutyric acid (GABA) (37) and the pituitary adenylate cyclase-activating polypeptide (38), the vast majority of RGC axon terminals release the excitatory neurotransmitter glutamate (39). Thus, we recorded excitatory postsynaptic currents (EPSCs) in a number of vLGN neurons by optogenetic activating presynaptic terminals of RGCs in the vLGN. The mean latency of optogenetic-evoked EPSCs (oEPSCs) was  $8.46 \pm 0.48$  ms (*n* = 6), which falls in the well-established range of monosynaptic connection (40). To further confirm the monosynaptic connection, we used

tetrodotoxin (TTX)/4-aminopyridine (4-AP) methods (41). The oEPSCs were completely abolished by the voltage-gated  $\text{Na}^+$  channel blocker TTX (1  $\mu$ M) that blocks generation and propagation of action potentials (APs) but then reappeared when 4-AP (100  $\mu$ M), a voltage-gated  $\text{K}^+$  channel blocker, was used in the presence of TTX (Fig. 5C) (41, 42). These results indicate that the oEPSCs were elicited by direct synaptic connections between RGCs and vLGN neurons. Behavioral results revealed that the optogenetic activation of RGC terminals in the vLGN reduced CFA-induced thermal hyperalgesia and mechanical allodynia (Fig. 5, D and E, and fig. S7, A to D). These findings imply that activation of

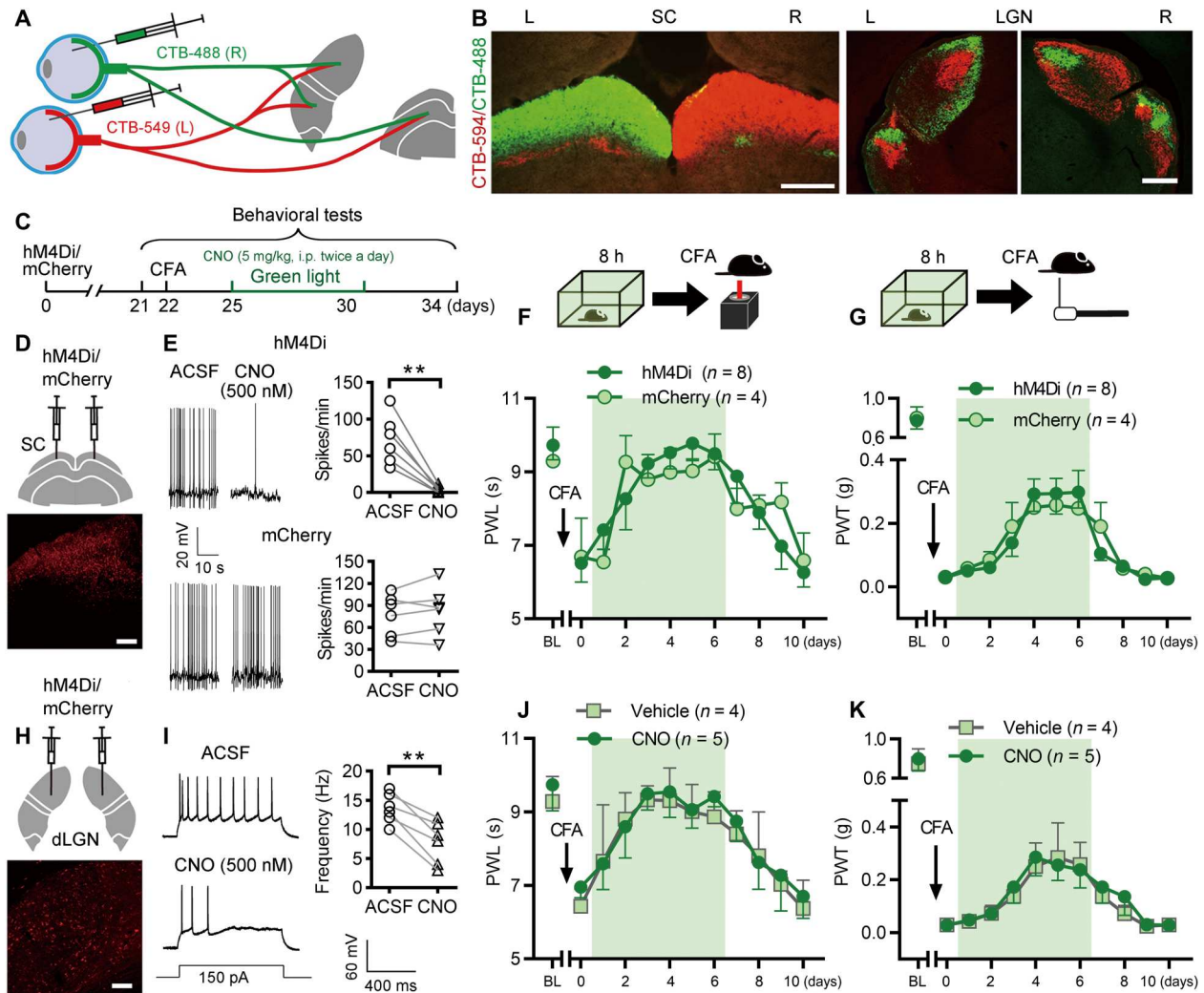


**Fig. 3. Inhibition of SC and dLGN neurons did not affect green light analgesia.** (A) Schematic showing Alexa Fluor 488/594-conjugated cholera toxin subunit B (CTB) injection into the vitreous cavity for tracing the retino-lateral geniculate nucleus (LGN) and retino-superior colliculus (SC) projections. (B) Photomicrograph of coronal section showing fluorescent signals in the bilateral SC and LGN [including dorsal part LGN, dLGN, and vLGN] after CTB-488/594 injection. Scale bar, 100  $\mu$ m. (C) Schematic of the protocol in experiments (D) to (K). (D) Schematic and photomicrograph showing AAV-Syn-hM4Di-mCherry/mCherry bilateral injection into the SC. Scale bar, 100  $\mu$ m. (E) Effect of bath CNO on mCherry<sup>+</sup> neuronal action potentials (APs) firing in SC slices from mice injected with AAV-hM4Di-mCherry and AAV-mCherry. (F and G) Effect of inhibiting SC neurons by chemogenetic manipulation on green light analgesia. (H) Schematic and photomicrograph showing AAV-Syn-hM4Di-mCherry bilateral injection into the dLGN. Scale bar, 100  $\mu$ m. (I) Effect of bath CNO on mCherry<sup>+</sup> neuronal AP firing in dLGN slices from AAV-hM4Di-mCherry-injected mice. (J and K) Effect of inhibiting dLGN neurons by chemogenetic manipulation on the green light analgesia. Two-way RM ANOVA (F, G, J, and K). Data are expressed as means  $\pm$  SEM. Sample sizes are indicated in parentheses. ACSF, artificial cerebrospinal fluid.

retino-vLGN projections could sufficiently alleviate arthritic pain, providing a neural-circuit basis for the green light analgesia.

Retrograde tracing by injection of retro-mCherry virus into the vLGN showed that vLGN-projecting RGCs included both non-photosensitive cRGCs and ipRGCs (Fig. 5, F to H). A Cre-off ChR2-mCherry (DO-ChR2-mCherry) virus was injected bilaterally into the vitreous cavity of *Opn4*-Cre mice to activate all RGCs except ipRGCs, and optical fibers were implanted into the vLGN (Fig. 5, I and J). The optogenetic activation of non-ipRGC retinal axons in the vLGN suppressed the CFA-induced thermal hyperalgesia and mechanical allodynia, suggesting that vLGN-projecting cRGCs (but not ipRGCs) might be involved in nociceptive modulation (Fig. 5, K to M). In addition, fiber photometry revealed that

green light exposure evoked increased  $\text{Ca}^{2+}$  signals in vLGN neurons that expressed the  $\text{Ca}^{2+}$  indicator, GCaMP6f (fig. S8, A to F). The elevated vLGN neuronal activity after green light exposure was also confirmed by increased expression of c-Fos (fig. S8, G and H).

### Enkephalinergic neurons and ENK in the vLGN contributed to green light analgesia

The vLGN contains a large number of GABAergic neurons (19, 43). A subset of GABAergic neurons, *Penk*<sup>+</sup> (encodes proenkephalin, PENK) GABAergic neurons, in the external vLGN have been identified as retina-innervated neurons (26). Therefore, we investigated the role of *Penk*<sup>+</sup> neurons located in the vLGN (vLGN<sup>Penk</sup>) in green

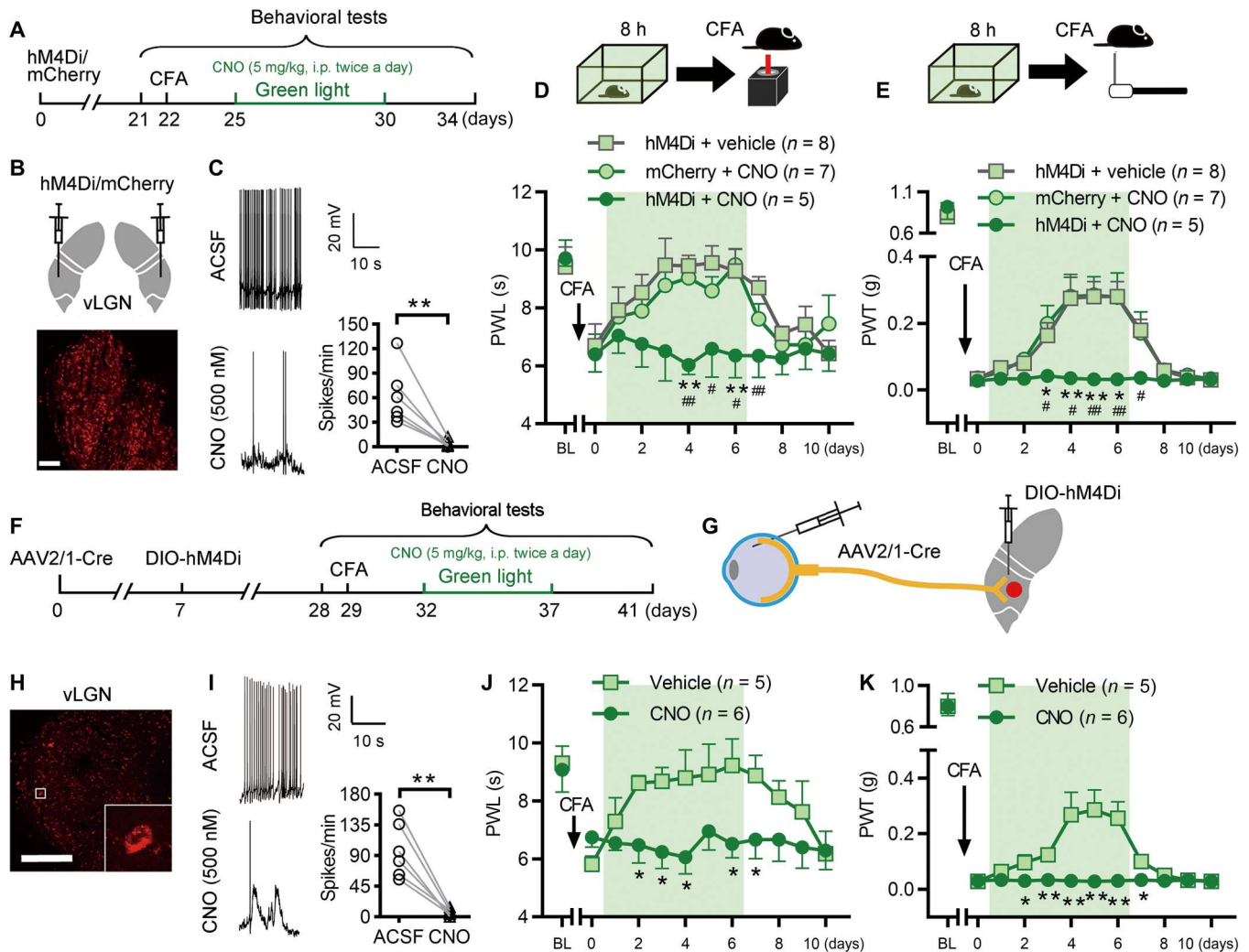


**Fig. 4. Inhibition of vLGN neurons and retino-vLGN projection blocked green light analgesia.** (A) Schematic of the protocol in experiments (D) and (E). (B) Schematic and photomicrograph showing AAV-Syn-hM4Di-mCherry/mCherry bilateral injection into the vLGN. Scale bar, 100  $\mu$ m. (C) Effect of bath CNO on AP firing in vLGN slices from AAV-hM4Di-mCherry-injected mice. (D and E) Effect of inhibiting vLGN neurons by chemogenetic manipulation on green light analgesia. \* $P$  < 0.05 and \*\* $P$  < 0.01 versus vehicle control; # $P$  < 0.05 and ## $P$  < 0.01 versus mCherry control. (F) Schematic of the protocol in experiments (J) and (K). (G) Schematic showing AAV2/1-Cre bilateral injection into the vitreous cavity and AAV-DIO-hM4Di-mCherry bilateral injection of the vLGN to infect retina-vLGN postsynaptic neurons with hM4Di specifically. (H) Photomicrograph showing the vLGN neurons receiving retinal projections. Scale bar, 100  $\mu$ m. (I) Effect of bath CNO on AP firing in vLGN slices from AAV2/1-Cre- and AAV-DIO-hM4Di-mCherry-injected mice. (J and K) Effect of inhibiting retino-vLGN postsynaptic neurons by chemogenetic manipulation on green light analgesia. \* $P$  < 0.05 and \*\* $P$  < 0.01 versus vehicle. Two-way RM ANOVA followed by post hoc Student-Newman-Keuls test (D, E, J, and K). Data are expressed as means  $\pm$  SEM. Sample sizes are indicated in parentheses.

light analgesia. Consistent with the previous findings, RNAscope in situ hybridization (ISH) revealed marked enrichment of *vGat*<sup>+</sup> GABAergic neurons in the vLGN; about 32% of GABAergic neurons were *Penk*<sup>+</sup> cells (Fig. 6A and fig. S9A). To determine whether vLGN<sup>Penk</sup> neurons were required for green light analgesia, we first ablated vLGN<sup>Penk</sup> neurons by injection of DIO-taCasp3-enhanced green fluorescent protein (EGFP) (44) or DIO-EGFP virus into the vLGN of *Penk*-Cre mice. The analgesic effects of green light were efficiently blocked by vLGN<sup>Penk</sup> neuron ablation (two-way RM ANOVA; PWLs:  $F_{1,9} = 21.9$ ,  $P = 0.001$ ; PWTs:  $F_{1,9} = 29.7$ ,  $P = 0.0004$ , Fig. 6, B to G). Subsequently, we examined the effects of *Penk* knockdown in vLGN neurons on green light analgesia. Lentivirus (Lv)-expressing *Penk*-short hairpin RNA (shRNA) was

injected into the vLGN to knock down *Penk* and inhibit the expression of PENK, the precursor protein of an endogenous opioid peptide, ENK, which produces analgesic effects by binding to  $\delta$ - and  $\mu$ -opioid receptors. The control group was injected with Lv-expressing EGFP (Fig. 6H). ISH and real-time polymerase chain reaction (PCR) analysis showed that the *Penk* mRNA expression was successfully suppressed at 2 weeks after treatment with Lv-expressing *Penk*-shRNA (Fig. 6, I and J). Green light analgesia in arthritic mice was prevented by *Penk* knockdown in the vLGN (two-way RM ANOVA; PWLs:  $F_{1,14} = 14.6$ ,  $P = 0.002$ ; PWTs:  $F_{2,14} = 13.4$ ,  $P = 0.003$ ; Fig. 6, L and M). In addition, systemic application of naloxone, an opioid receptor antagonist (5 mg/kg, i.p.), completely reversed the analgesic effects induced by chemogenetic activation of



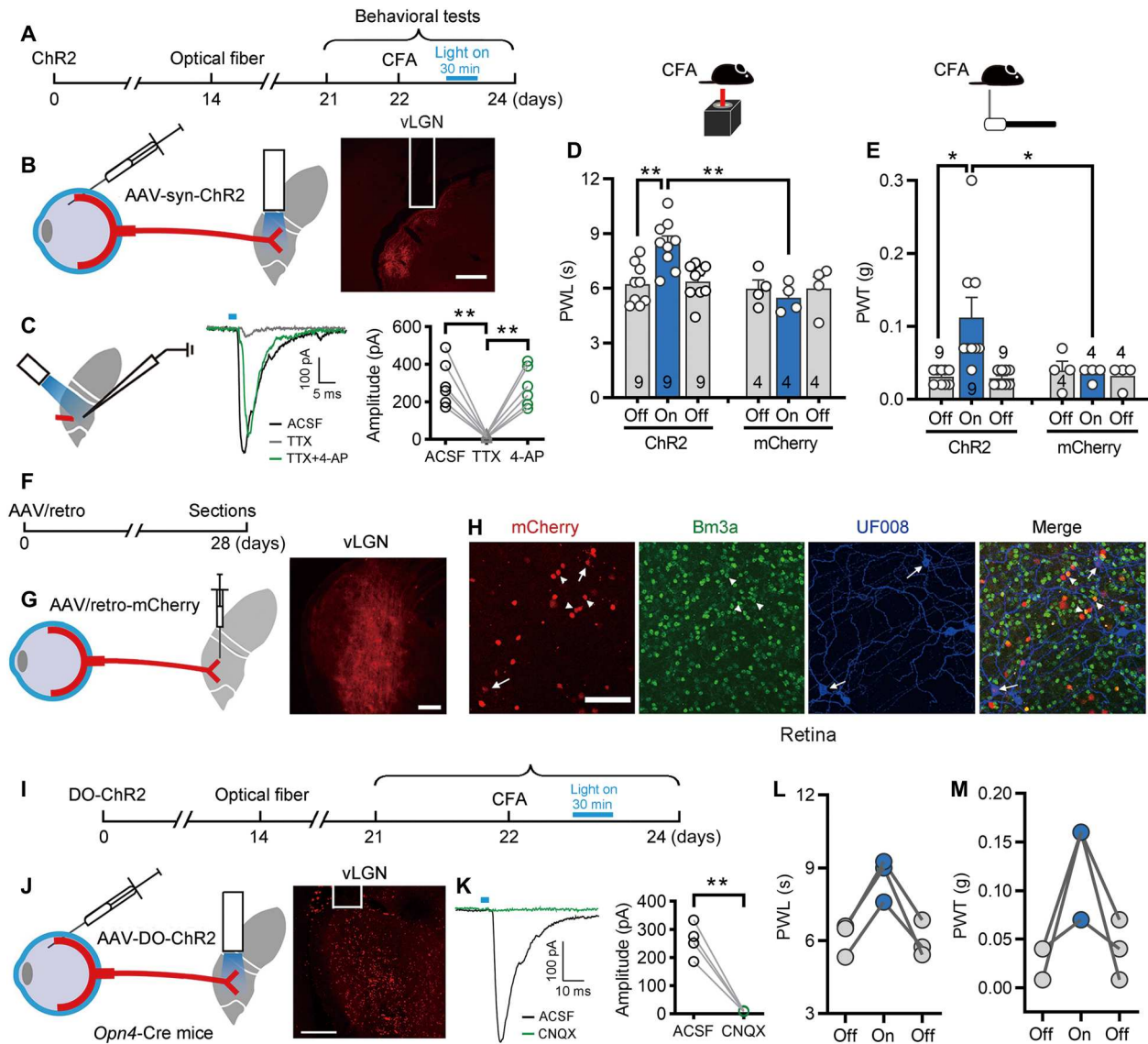


**Fig. 5. Activation of retina-vLGN projections suppressed CFA-induced hyperalgesia and allodynia.** (A) Schematic of the protocol in experiments (B) to (E). (B) Schematic and photomicrograph showing channelrhodopsin-2 (ChR2)-positive RGC terminals in the vLGN. Scale bar, 250  $\mu$ m. (C) Representative traces and summary data showing oEPSCs evoked by blue light stimulation of the RGC terminals in the vLGN. (D and E) Effect of activating retino-vLGN projections by optogenetic manipulation on CFA-induced thermal hyperalgesia (D) and mechanical allodynia (E). \* $P < 0.05$  and \*\* $P < 0.01$  versus light off. (F) Schematic of the protocol in experiments (G) and (H). (G) Schematic and photomicrograph showing retro-AAV-mCherry injection into the vLGN to label vLGN-projecting RGCs. Scale bar, 100  $\mu$ m. (H) Retrograde tracing showing vLGN-projecting cRGCs (Brn3a) and ipRGC (UF008). Scale bar, 100  $\mu$ m. (I) Schematic of the protocol in experiments (J) to (M). (J) Schematic and photomicrograph showing AAV-DO-ChR2-mCherry injection into the vitreous cavity of *Opn4*-Cre mice and ChR2-positive cRGCs terminals in the vLGN. Scale bar, 100  $\mu$ m. (K) Representative traces and summary data showing oEPSCs evoked by blue light stimulation of cRGC terminals in the vLGN. (L and M) Effect of activating the retino<sup>cRGC</sup>-vLGN pathway by optogenetic manipulation on arthritic pain in three mice. One-way ANOVA followed by post hoc Student-Newman-Keuls test (D and E). Data are expressed as means  $\pm$  SEM. Sample sizes are indicated in bars. TTX, tetrodotoxin; 4-AP, 4-aminopyridine; CNQX, 6-cyano-7-nitro-quinoxaline-2,3-dione.

vLGN neurons; this finding supported the involvement of central opioid circuits (fig. S9, B to F). As mentioned above, the activation of retino-vLGN projections directly inhibited CFA-induced thermal hyperalgesia and mechanical allodynia. To determine whether vLGN<sup>Penk</sup> neurons were involved in this effect, Syn-ChR2-enhanced yellow fluorescent protein virus was injected bilaterally into the vitreous cavity; Cre-dependent MAC (a blue light-sensitive proton pump that enables neural silencing derived from the fungus *Leptosphaeria maculans*)-mCherry or DIO-mCherry

(control) was injected bilaterally into the vLGN of *Penk*-Cre mice (Fig. 7A). Thus, blue light (470 nm, 20 Hz, 25 ms, 5 mW, 30 min) simultaneously activated activated retino-vLGN projection terminals and inhibited vLGN<sup>Penk</sup> neurons (Fig. 7, B and C). Selective inhibition of vLGN<sup>Penk</sup> neurons completely blocked the analgesic effects induced by activation of retino-vLGN projections (one-way ANOVA; PWTs:  $F_{5,18} = 5.0$ ,  $P = 0.0049$ ; PWTs:  $F_{5,18} = 10.5$ ,  $P < 0.0001$ ; Fig. 7, D to F). A recent study showed that vLGN/intergeniculate leaflet (IGL) GABAergic neurons were involved in bright

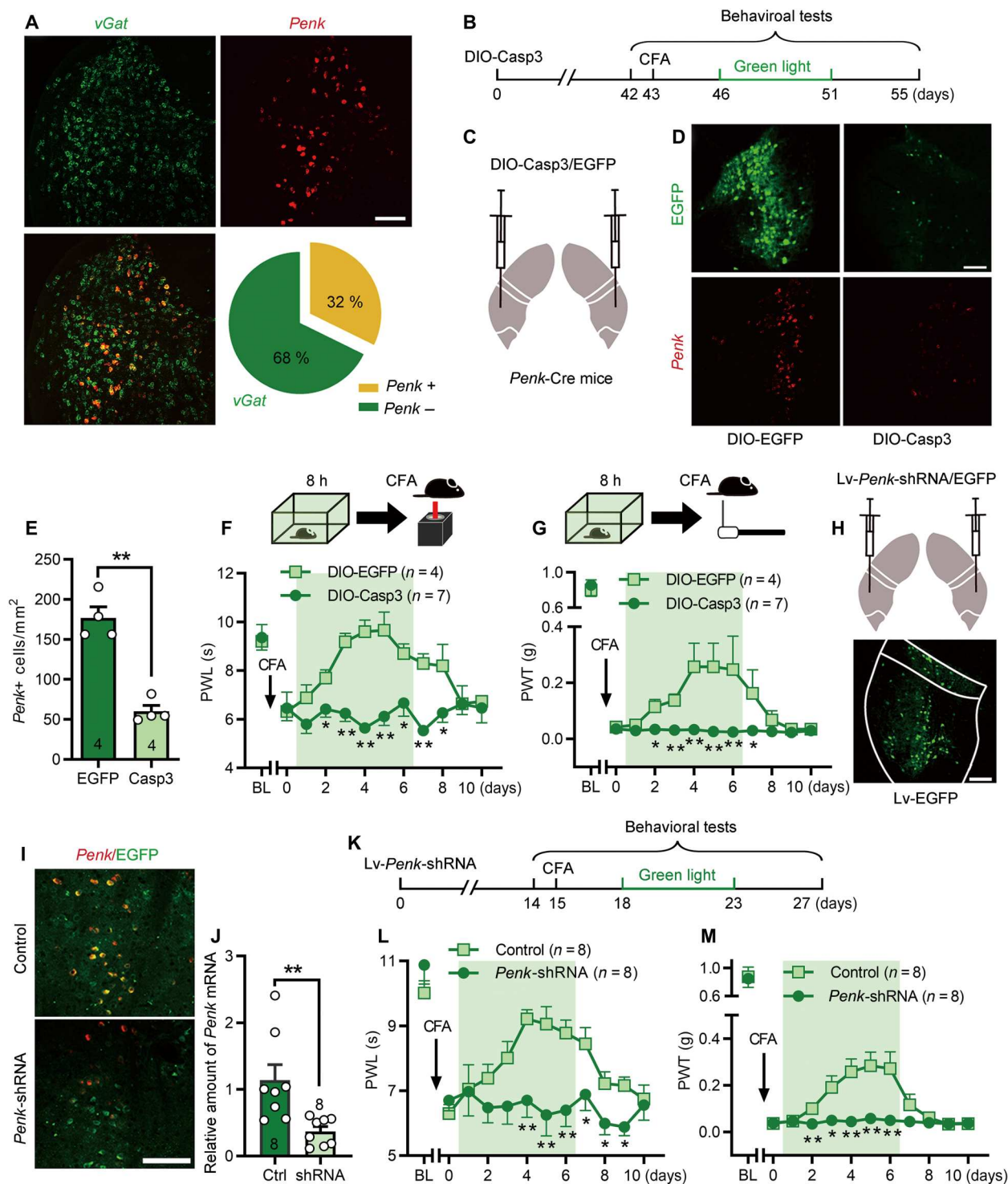


**Fig. 6. *Penk*<sup>+</sup> neurons and ENK in the vLGN contributed to green light analgesia.** (A) In situ hybridization (ISH) showing colocalization and proportion of *Penk* mRNA with *vGat* mRNA. (B) Schematic of the protocol in experiments (C) to (G). (C) Schematic showing AAV-DIO-Casp3-EGFP/AAV-DIO-EGFP injection into the vLGN of *Penk*-Cre mice. (D and E) ISH showing *Penk* mRNA and EGFP-positive neurons in the vLGN after DIO-Casp3 injection. Scale bar, 100  $\mu$ m. (F and G) Effect of ablation of vLGN<sup>Penk</sup> neurons by Casp3 virus on green light analgesia. \* $P < 0.05$  and \*\* $P < 0.01$  versus EGFP control. (H) Schematic and photomicrograph showing Lv-expressing *Penk*-shRNA injection into the vLGN. Scale bar, 100  $\mu$ m. (I) ISH showing *Penk* mRNA-positive signals in the vLGN<sup>Penk</sup> neurons after *Penk* knockdown. Scale bar, 100  $\mu$ m. (J) Real-time PCR showing relative *Penk* mRNA expression in the vLGN. PCR analysis was performed at least three times, and similar results were obtained. (K) Schematic of the protocol in experiments (L) and (M). (L and M) Effect of knocking down *Penk* in the vLGN on green light analgesia. \* $P < 0.05$  and \*\* $P < 0.01$  versus control. Two-tailed Student's *t* test (E and J), and two-way RM ANOVA followed by post hoc Student-Newman-Keuls test (F, G, L, and M). Data are expressed as means  $\pm$  SEM. Sample sizes are indicated in parentheses.



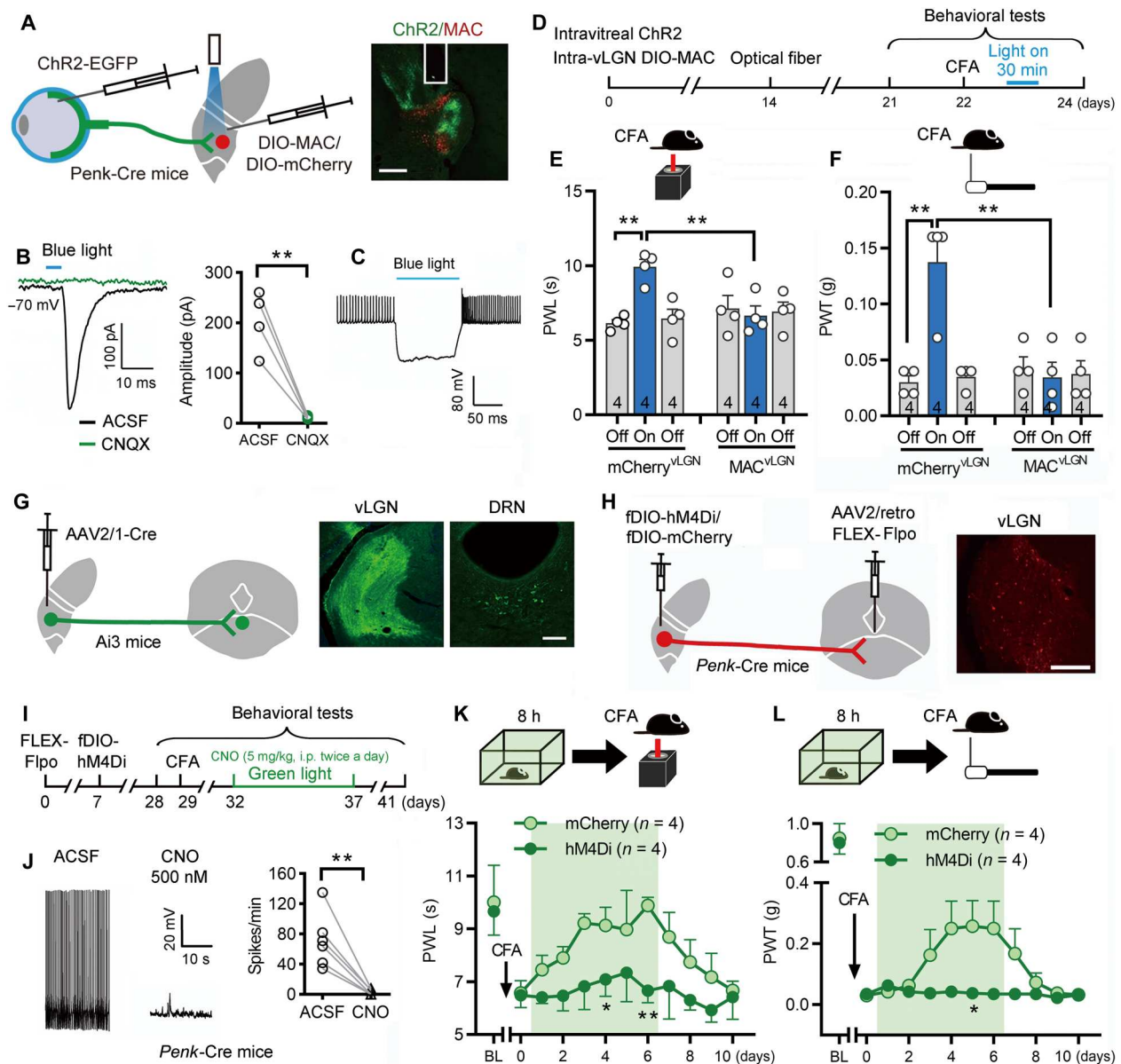


**Fig. 7. Retino-vLGN<sup>Penk</sup>-DRN pathway contributed to green light analgesia.** (A) Schematic and photomicrograph showing RGC terminals (green) and Penk<sup>+</sup> neurons (red) in the vLGN. Scale bar, 250  $\mu$ m. (B) Representative traces and summary data showing oEPSCs evoked by blue light stimulation of RGC terminals in vLGN neurons. (C) Representative trace showing the effect of blue light stimulation on a vLGN<sup>Penk</sup> neuron expressing leptosphaeria maculans (MAC)-mCherry. (D) Schematic of the protocol in experiments (E) and (F). (E and F) Effect of activating retino-vLGN projections by optogenetic manipulation on CFA-induced hyperalgesia (E) and allodynia (F). \*\* $P < 0.01$  versus light off. (G) Schematic and photomicrograph showing AAV2/1-Cre injected into the vLGN of Ai3 mice, and postsynaptic neurons receiving vLGN neuronal projections in the dorsal raphe nucleus (DRN). Scale bar, 100  $\mu$ m. (H) Schematic and photomicrograph showing DRN-projecting vLGN<sup>Penk</sup> neurons. Scale bar, 200  $\mu$ m. (I) Schematic of the protocol in experiments (K) and (L). (J) Effect of bath CNO on AP firing of vLGN<sup>Penk</sup> neuron expressing hM4Di in Penk-Cre mice. (K and L) Effect of inhibiting DRN-projecting vLGN<sup>Penk</sup> neurons by chemogenetic manipulation on green light analgesia. \* $P < 0.05$  and \*\* $P < 0.01$  versus control.  $P$  values were determined by one-way (E and F) and two-way RM ANOVA (K and L) followed by post hoc Student-Newman-Keuls test. Sample sizes are indicated in bars and parentheses.

white light (3000 lux)-induced analgesia (20). We therefore tested whether vLGN enkephalinergic neurons also contribute to bright light analgesia. Consistent with the previous study, we found that bright white light (3000 lux, 2 hours/day) exposure for 7 days attenuated arthritis-induced hyperalgesia and allodynia. However, chemogenetic inhibition of vLGN<sup>Penk</sup> neurons had no effect on bright light analgesia (fig. S10), suggesting that this subclass of

vLGN GABAergic neurons specifically participate in green light analgesia.

### vLGN<sup>Penk</sup>-DRN pathway was involved in green light analgesia

A previous study of efferent projections from the rat vLGN implied that vLGN neurons project to the DRN (45), an important nucleus

related to descending pain modulation (46). We also observed such projections in mice. We injected recombinant AAV1-Cre (rAAV-hSyn-Cre) bilaterally into the vLGN of Ai3 mice to infect postsynaptic neurons in efferent regions of vLGN; we detected fluorescence signals in the DRN (Fig. 7G). To verify the effects of the vLGN-DRN pathway on green light analgesia, we used a Cre-enabled chemogenetic inhibition system that involved injection of retrograde virus-expressed FLEX-FlpO bilaterally into the DRN and Flp-dependent hM4Di (fDIO-hM4Di-mCherry) bilaterally into the vLGN of *Penk*-Cre mice (Fig. 7, H and I). Thus, we achieved selective inhibition of DRN-projecting *Penk*<sup>+</sup> neurons in the vLGN by injecting CNO. Chemogenetic inhibition of vLGN<sup>Penk</sup>-DRN inputs significantly blocked green light analgesia in CFA-arthritic mice (two-way RM ANOVA; PWLs:  $F_{1,6} = 6.7$ ,  $P = 0.04$ ; PWTs:  $F_{1,6} = 11.4$ ,  $P = 0.015$ ; Fig. 7, J to L). Furthermore, we used optogenetic manipulation to investigate whether activation of the vLGN<sup>Penk</sup>-DRN circuit directly produced analgesia via bilateral injection of Cre-dependent ChR2-mCherry virus into the vLGN of *Penk*-Cre mice (Fig. 8, A to C). Optogenetic activation of vLGN<sup>Penk</sup> terminals in the DRN significantly alleviated CFA-induced thermal hyperalgesia (two-way ANOVA,  $F_{1,10} = 5.1$ ,  $P = 0.048$ ; Fig. 8D). This effect was blocked by pretreatment of the DRN with D-Phe-Cys-Tyr-D-Trp-Arg-Thr-Pen-Thr-NH<sub>2</sub> (CTAP; 150 ng), a  $\mu$ -opioid receptor antagonist, but not by pretreatment with naltrindole (NTI; 450 ng), a  $\delta$ -opioid receptor antagonist (Fig. 8E), implying that ENK and  $\mu$ -

opioid receptors mediated the analgesia caused by vLGN<sup>Penk</sup>-DRN pathway activation. At the same dose without blue light stimulation, CTAP and NTI per se had no effects on CFA-induced hyperalgesia (Fig. 8F).

## DISCUSSION

In the past decade, numerous preclinical and clinical studies have reported pain modulation by light. Depending on the wavelength, intensity, and route of administration, light has distinct regulatory effects on pain. For example, green light exposure markedly reduces pain during an acute migraine episode compared to other chromatic lights (such as white, blue, amber, and red) (22). A recent study reported that green light exposure effectively reduced the number of headache days in patients with migraine and pain intensity in patients with fibromyalgia (8, 12, 13). In a preclinical study that used colored contact lenses as filters, repeated green light exposure produced antinociception in rats; this effect required engagement of the visual system (11). However, it was unclear how the visual system drives the analgesic effect of green light. In this study, we found that retinal cone photoreceptors are essential for green light analgesia, whereas rods play a secondary role, as demonstrated by the complete and partial elimination of this effect after genetic ablation of cones and rods, respectively. In addition, ablation of ipRGCs, which are widely presumed to participate in non-imaging-forming vision,

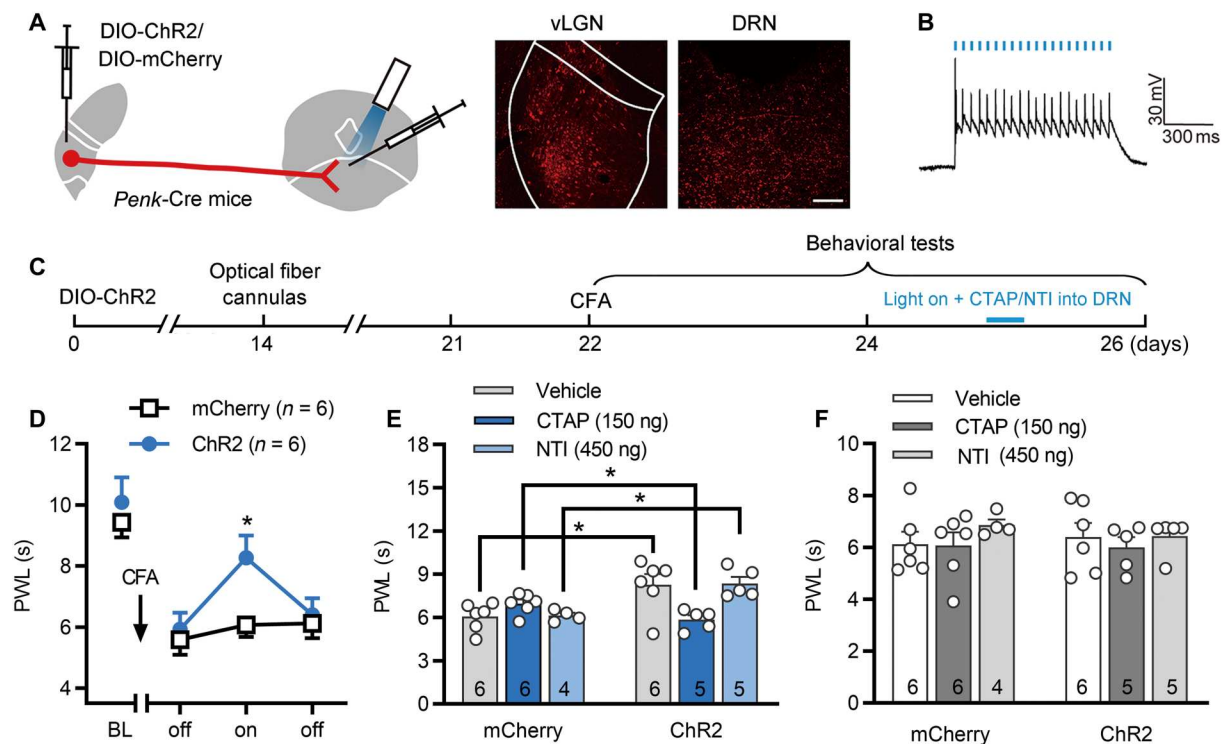


**Fig. 8. Activation of vLGN<sup>Penk</sup>-DRN projection suppressed CFA-induced hyperalgesia through Mu opioid receptor.** (A) Schematic and photomicrograph showing intra-vLGN injection of DIO-ChR2-mCherry in *Penk*-Cre mouse and vLGN<sup>Penk</sup> terminals in the DRN. Scale bar, 100  $\mu$ m. (B) An example showing blue light stimulation-evoked APs in vLGN<sup>Penk</sup> neurons expressing ChR2-mCherry. (C) Schematic of the protocol in experiments (D) to (F). (D) Effect of activating vLGN<sup>Penk</sup>-DRN projections by optogenetic manipulation on CFA-induced hyperalgesia during light application. \* $P < 0.05$  versus mCherry control. (E) Effect of activating vLGN<sup>Penk</sup>-DRN pathway by optogenetic manipulation on CFA-induced hyperalgesia after intra-DRN administration of CTAP ( $\mu$ -opioid receptor antagonist) or naltrindole (NTI) hydrochloride ( $\delta$ -opioid receptor antagonist). \* $P < 0.05$ . (F) Effect of intra-DRN application of CTAP or NTI on CFA-induced hyperalgesia. Two-way RM ANOVA (D) and one-way ANOVA (E to G) followed by post hoc Student-Newman-Keuls test. Sample sizes are indicated in bars.

did not affect green light analgesia. Moreover, we found that the analgesic effect of green light was dependent on the retinal RGC-vLGN<sup>Penk</sup>-DRN circuits (fig. S11).

Light affects biological processes in humans and animals through the integumentary and visual systems. The analgesic effects of bright white, green, blue, red, and near-infrared lights have been documented (20, 21, 47). Red (625 to 740 nm) and near-infrared (750 to 1000 nm) lights have high tissue penetration and are used to treat various pain disorders by cutaneous application (48–50). Because of the shorter wavelengths, green light analgesia does not appear to influence the integumentary system. In this study, ablation of cones and rods completely blocked the analgesic effect of green light, implying that the visual pathway has a crucial role. White light has a broad spectrum; it contains multiple wavelengths. Thus, bright white light analgesia may be the cumulative effect of different wavelengths. Considering that bright light therapy is typically applied at 3000 to 5000 lux (20, 21, 51), this may cause stress in nocturnal rodents (52), exacerbate headaches (53), and potentially induce retinal degeneration (54–58). Here, we used low-illuminance green light, which is sufficient to excite rods and cones (59) and might have lower risk of adverse effects.

Cone and rod photoreceptors are regarded as the first components of the retinal visual pathway. These cells capture visual information and ultimately respond to light (14). Visual phototransduction relies on the absorption of photons by visual opsins that are expressed in photoreceptors. Most mouse cones co-express both short wavelength-sensitive opsin and middle wavelength-sensitive opsin in a dorsal-ventral gradient (60); they exhibit varying degrees of responsiveness to green light stimulation. Consequently, most RGCs (retinal output neurons driven by photoreceptors that convey photo signals to higher visual centers) can be excited by green light (61, 62). In addition, we found that green light analgesia was completely abolished in cone-deficient mice, strongly implying a key role for cones in this analgesic effect. Mouse rods exhibit peak sensitivity to light at about 500 nm (63, 64), a wavelength present in the green range. In this study, we found that rod-specific genetic dysfunction led to weaker green light analgesia, supporting the idea that rod-mediated signals were partially involved in this effect. On the basis of these findings, we speculate that a specific group of RGCs that receive rod-cone mixed inputs but are primarily driven by cones were the retinal conduits of the neural circuit underlying green light analgesia. In addition to rods and cones, ipRGCs constitute a third class of retinal photoreceptors that play vital roles in non-image-forming visual processes, such as pupil constriction, circadian rhythms, memory (18), mood (19), and migraine-related photophobia (65). Therefore, we also examined the role of ipRGCs in green light analgesia. Although ipRGCs contribute to the antinociceptive effects of bright white light (20), our findings indicate that they are not involved in green light analgesia.

Many brain regions receive afferent input from the retina. Some non-image-forming visual centers receive afferent input from both cRGC and ipRGCs (66), suggesting that cRGCs may participate in non-image-forming vision. Many RGCs innervate the LGN (67), which is an important part of the visual thalamus; in rodents, the LGN is divided into the dLGN, vLGN, and IGL. Nucleus-specific differences in nerve terminal composition, distribution, and morphology have been found among the three subnuclei (67–69). The IGL/vLGN is reportedly involved in the regulation of anxiety,

depression, spatial memory, and pain (19, 20). In this study, we found that the RGC-vLGN projections mediated green light analgesia. Moreover, optical fiber calcium imaging and c-Fos immunohistochemical experiments showed that green light exposure directly activated vLGN neurons; these findings indicate that the vLGN may also be involved in chromatic identification. Furthermore, previous work observed strong blue opsin preference in the lateral vLGN and strong green opsin preference in the medial vLGN in mice (70). Thus, we can speculate that vLGN neurons located in the medial subsection of this area might be involved in green light analgesia.

The vLGN is enriched in GABAergic neurons, which provide inhibitory modulation to various brain areas, including the olivary pretectal nucleus, lateral habenula, and ventrolateral periaqueductal gray (vlPAG) (19, 20, 24). Our data show that about 32% of vGat<sup>+</sup> vLGN neurons were *Penk*<sup>+</sup>; such neurons project to the DRN, an important brain region involved in endogenous descending pain control (71). PENK is the precursor protein of ENK, which has two natural subtypes: leu-ENK and met-ENK. ENK is an agonist of the  $\delta$ -opioid receptor and a weak agonist of the  $\mu$ -opioid receptor (72, 73). To assess the contribution of ENK in the vLGN to green light analgesia, we used shRNA to knock down ENK in the vLGN; we also selectively ablated vLGN<sup>Penk</sup> neurons by injecting DIO-taCasp3 virus into *Penk*-Cre mice. We found that vLGN<sup>Penk</sup> neurons and the ENK that they synthesized played key roles in green light analgesia mediated by retino-vLGN projections. In particular, activation of DRN-projecting vLGN<sup>Penk</sup> axons robustly alleviated CFA-induced hyperalgesia, and inhibition of this pathway effectively prevented green light analgesia. Furthermore, pretreatment with a  $\mu$ -opioid receptor antagonist in the DRN effectively blocked the analgesic effects induced by activating vLGN<sup>Penk</sup>-DRN projections, implying that ENK from the vLGN to the DRN produces analgesia that is mediated by modulation of  $\mu$ -opioid receptor activity in the DRN.  $\mu$ -Opioid receptors are reportedly widely distributed in DRN neurons, especially GABAergic neurons, implying that  $\mu$ -opioid receptors excite descending projection neurons (such as 5-hydroxytryptamine neurons) by reducing GABAergic tone (74).  $\mu$ -Opioid receptors in the PAG/DRN region have been shown to produce analgesia by inhibiting GABAergic function in the vlPAG/DRN region (75). Because few  $\delta$ -opioid receptors are present in the DRN (76, 77), it is expected that vLGN<sup>Penk</sup>-DRN pathway-mediated analgesia was not inhibited by treatment with a  $\delta$ -opioid receptor antagonist. Together, our results strongly indicate that cone/rod-RGC-vLGN<sup>Penk</sup>-DRN circuits are required for green light analgesia.

It should be mentioned that recent work reported a retina-initiated pathway mediating the antinociceptive effect of bright white light (20), which appears to be somewhat similar to the circuits we described here for green light analgesia. For example, both studies have revealed a vital role of retina-innervated vLGN neurons in phototherapy analgesia. However, the differences in the characterized neural circuits between these two works are rather clear. First, the retinal conduits mediating green light analgesia reported here are likely to be cRGCs that are driven by cone-dominated inputs, whereas those responsible for bright light antinociception previously reported are mostly (~82%) M4-type ipRGCs [SMI-32 (an antibody which recognizes the nonphosphorylated epitopes on the neurofilament proteins) positive ON-type RGCs] (78, 79). Second, although both the DRN and vlPAG



receive projections from the vLGN and participate in pain modulation, their cytoarchitectonic and input/output profiles are quite different. For instance, it is well established that DRN serotonergic neurons directly project to the spinal dorsal horn, inhibiting nociceptive transmission, whereas the vPAG-mediated antinociception is mainly relayed via the RVM and A7 nuclei (80). Third, in this study, at least one confined subclass of vLGN neurons, the enkephalinergic neurons and  $\mu$ -opioid receptor in DRN neurons, is found to be involved in green light analgesia. Our results showed that chemogenetic inhibition of vLGN<sup>Penk</sup> neurons did not affect bright light analgesia, raising the possibility that the vLGN<sup>Penk</sup>-DRN pathway specifically mediated green light analgesia.

The interaction of multiple sensory systems (such as vision, olfactory, gustatory, auditory, and somatosensory) is vital for survival from an evolutionary standpoint. Previous studies have demonstrated that pain, olfactory, and gustatory sensory-processing pathways interact at both peripheral and central systems (81). Equal intensities of painful stimuli were perceived to be weaker when sweet odors and substances were administered than when bitter substances were administered (82). Green light analgesia may partially arise from the interaction between visual and somatosensory systems. Our findings in mice without a cerebral cortex might be explained by functional connectivity among primary somatosensory, visual, auditory cortex, and other cortical areas (such as prefrontal cortex) that participate in cross-modal processing (83).

Although various light wavelengths have been used to treat several medical conditions, green light might have provided improved health and safety benefits for humans and animals from an evolutionary perspective. Exposure to an environment rich in the color green (such as forest bathing) can decrease physiological and psychological pain (84). Psychology studies have shown that "green" conveys positive information related to happiness (85). When participants were shown a color before pain stimulation, pain intensity scores were higher than baseline values for all colors, except green (86, 87). A clinical study also showed that green light was less likely than other wavelengths of light to exacerbate migraine headache; it even alleviated headache at low intensities (22). Although it is unclear whether color perception is comparable between humans and rodents, green light exposure in both humans and rodents reduces pain sensitivity, suggesting the involvement of shared mechanisms between the two species. Therefore, it may be clinically useful to investigate the potential mechanisms of green light analgesia, which is simple, safe, and economical.

This study has several limitations. For example, after melanopsin-SAP treatment, a few ipRGCs were spared, and their possible contribution to green light analgesia cannot be completely excluded; meanwhile, melanopsin-SAP preferentially ablates M1 to M3 cells, leaving M4 to M6 cells largely intact (88, 89). Thus, more effective technical methods that enable a thorough ablation of ipRGCs of all subtypes (90) could be used in future work to resolve this issue. In addition, besides PENK<sup>+</sup> neurons, *Ecel1*<sup>+</sup> (endothelin converting enzyme like 1), *Pvalb*<sup>+</sup> (Parvalbumin), and *Spp1*<sup>+</sup> (Osteopontin) retina-innervated cells have also been identified in the vLGN (26). Further study is needed to determine whether other subclasses of vLGN neurons participate in green light analgesia. Last, the analgesic effect of green light was absent in *Tra2b* conditional knockout mice with major cortex loss, implying that some cortical circuits may also be required for green light analgesia. It remains to be

determined which cortical structures and related circuits are involved in the green light analgesia.

## MATERIALS AND METHODS

### Study design

The main goal of this study was to investigate the visual circuits that underlie low-intensity green light-induced analgesia, and the results were expected to provide insights into potential strategies for the chronic pain management. We first confirmed the analgesic effect of repeated low-intensity green light exposure in CFA-induced arthritis mice. Then, we characterized the retinal photoreceptors responsible for this effect using three mouse models in which cones, rods, or ipRGCs were genetically or pharmacologically ablated. Next, we assessed the retinal recipients responsible for the green light analgesia by conducting chemogenetic inhibition of neurons in the dLGN, SC, and vLGN. Moreover, we checked the expression of *Penk* mRNA in *vGat*<sup>+</sup> GABAergic neurons in the vLGN by RNAscope ISH. Using shRNA and apoptosis induction techniques, we affirmed that ENK and vLGN<sup>Penk</sup> neurons were essential for green light analgesia. Last, using circuit tracing and optogenetic/chemogenetic manipulation, we examined the role of the vLGN<sup>Penk</sup>-DRN pathway in the green light analgesic effect. Mice were randomly assigned into different cages and groups and tested by an investigator blinded to mouse genotypes/treatments and group assignments. The sample sizes and power calculation were based on our previous knowledge and experience with similar experimental models and anticipated biological variables. All experiments have been replicated successfully, and all data were included in analysis. Data were acquired and analyzed in a blinded manner. Sample sizes and replicates are shown in the figures or figure legends.

### LED light exposure

Laser-engraved LED light-guiding plates with adjustable brightness were installed in a three-dimensional printing frame that could cover the top and four walls of a mouse home cage (Institute of Semiconductors, Chinese Academy of Science). Mice were exposed to LED lights of various wavelengths with unlimited access to food and water in a custom-designed light-tight cabinet. Low-intensity light exposure began during the light phase and continued for 8 hours (8 a.m. to 4 p.m.) daily for 6 days; bright light exposure continued for 2 hours (1 to 3 p.m.) daily for 7 days. Behavioral assessment was performed after light exposure. At the end of daily behavioral testing, the mice were returned to their regular animal room (with ~200 lux white ambient illumination) until the next day.

### Mouse arthritis pain model

Mouse monoarthritis was induced by the intra-articular administration of CFA (25  $\mu$ l) unilaterally into the knee joints of mice under isoflurane anesthesia. Control mice received intra-articular injection of 25  $\mu$ l of sterile saline.

### von Frey test

Mechanical allodynia was assessed by measuring PWTs in response to a calibrated series of von Frey filaments (0.02 to 1.4 g; North Coast Med Inc.). Each mouse was placed in a chamber on an elevated metal mesh floor and then allowed to acclimatize for about 30

min. A series of von Frey filaments were then applied vertically to the central region of the hind paw plantar surface in ascending order (0.02, 0.04, 0.07, 0.16, 0.4, and 0.6 for model; 0.16, 0.4, 0.6, 1, and 1.4 for naive). Filaments were applied until buckling occurred and then maintained for about 2 s. A filament was applied only when the mouse was stationary and standing on all four paws. A withdrawal response was considered valid only if the hind paw was completely removed from the customized platform. Each filament was applied five times at 15-s intervals, and the minimum value that caused at least three responses was recorded as the PWT.

### Hargreaves' test

Thermal hyperalgesia was assessed by measuring PWLs in response to a radiant heat source (IITC Life Science). Mice were placed individually into Plexiglas chambers on an elevated glass platform and then allowed to acclimatize for 30 min. The heat source was maintained at a constant intensity, which produced a stable PWL of about 8 to 10 s in naive mice. The heat source was switched off when paw withdrawal occurred or after 20 s of emission. The time between the onset of radiant heat application and hind paw withdrawal was defined as the PWL. The hind paws were tested three times with 10-min intervals between the tests. The mean latency of the three trials was then calculated.

### Statistical analysis

The data are presented as the means  $\pm$  SEM. All data from the different groups were verified for normality and homogeneity of variance using Shapiro-Wilk and Levene's tests before analysis. For CFA-induced behavioral hypersensitivity, green light analgesic effects and chemogenetic manipulations were analyzed using two-way RM ANOVA following by post hoc Student-Newman-Keuls tests. The differences in immunoreactive/ISH signals and mRNA expression (real-time PCR) between treated groups were compared using Student's *t* test or Mann-Whitney *U* test (nonparametric data). Electrophysiological data were tested using paired *t* test. For optogenetic manipulation, PWL and PWT were compared using one-way ANOVA followed by post hoc Student-Newman-Keuls tests or Kruskal-Wallis *H* test (nonparametric data). No additional data were excluded from the statistical analyses because of outlier status. All analyses were two-tailed, and a *P* value of less than 0.05 was considered statistically significant. The statistical analyses were performed using GraphPad Prism 8.0 software (GraphPad Software).

### Supplementary Materials

#### This PDF file includes:

Materials and Methods  
Figs. S1 to S11  
Tables S1 and S2

#### Other Supplementary Material for this manuscript includes the following:

Data files S1 and S2  
MDAR Reproducibility Checklist

[View/request a protocol for this paper from Bio-protocol.](#)

### REFERENCES AND NOTES

1. N. Henschke, S. J. Kamper, C. G. Maher, The epidemiology and economic consequences of pain. *Mayo Clin. Proc.* **90**, 139–147 (2015).
2. Z. Xie, T. Fan, J. An, W. Choi, Y. Duo, Y. Ge, B. Zhang, G. Nie, N. Xie, T. Zheng, Y. Chen, H. Zhang, J. S. Kim, Emerging combination strategies with phototherapy in cancer nanomedicine. *Chem. Soc. Rev.* **49**, 8065–8087 (2020).
3. E. Racz, E. P. Prens, Phototherapy of psoriasis, a chronic inflammatory skin disease. *Adv. Exp. Med. Biol.* **996**, 287–294 (2017).
4. S. M. Faulkner, D. J. Dijk, R. J. Drake, P. E. Bee, Adherence and acceptability of light therapies to improve sleep in intrinsic circadian rhythm sleep disorders and neuropsychiatric illness: A systematic review. *Sleep Health* **6**, 690–701 (2020).
5. E. Pjrek, M.-E. Friedrich, L. Cambioli, M. Dold, F. Jäger, A. Komorowski, R. Lanzenberger, S. Kasper, D. Winkler, The efficacy of light therapy in the treatment of seasonal affective disorder: A meta-analysis of randomized controlled trials. *Psychother. Psychosom.* **89**, 17–24 (2020).
6. Y. P. Lin, Y. H. Su, S. F. Chin, Y. C. Chou, W. T. Chia, Light-emitting diode photobiomodulation therapy for non-specific low back pain in working nurses: A single-center, double-blind, prospective, randomized controlled trial. *Medicine* **99**, e21611 (2020).
7. Y.-C. Kuan, Low-level laser therapy for fibromyalgia: A systematic review and meta-analysis. *Pain Physician* **3**, 241–254 (2019).
8. L. F. Martin, A. M. Patwardhan, S. V. Jain, M. M. Salloum, J. Freeman, R. Khanna, P. Gannala, V. Goel, F. N. Jones-MacFarland, W. D. Killgore, F. Porreca, M. M. Ibrahim, Evaluation of green light exposure on headache frequency and quality of life in migraine patients: A preliminary one-way cross-over clinical trial. *Cephalalgia* **41**, 135–147 (2021).
9. A. L. M. de Andrade, P. S. Bossini, A. L. M. do Canto De Souza, A. D. Sanchez, N. A. Parizotto, Effect of photobiomodulation therapy (808 nm) in the control of neuropathic pain in mice. *Lasers Med. Sci.* **32**, 865–872 (2017).
10. H. Serrage, V. Heiskanen, W. M. Palin, P. R. Cooper, M. R. Milward, M. Hadis, M. R. Hamblin, Under the spotlight: Mechanisms of photobiomodulation concentrating on blue and green light. *Photochem. Photobiol. Sci.* **18**, 1877–1909 (2019).
11. M. M. Ibrahim, A. Patwardhan, K. B. Gilbraith, A. Moutal, X. Yang, L. A. Chew, T. Largent-Milnes, T. P. Malan, T. W. Vanderah, F. Porreca, R. Khanna, Long-lasting antinociceptive effects of green light in acute and chronic pain in rats. *Pain* **158**, 347–360 (2017).
12. L. F. Martin, A. Moutal, K. Cheng, S. M. Washington, H. Calligaro, V. Goel, T. Kranz, T. M. Largent-Milnes, R. Khanna, A. Patwardhan, M. M. Ibrahim, Green light antinociceptive and reversal of thermal and mechanical hypersensitivity effects rely on endogenous opioid system stimulation. *J. Pain* **22**, 1646–1656 (2021).
13. L. Martin, F. Porreca, E. I. Mata, M. Salloum, V. Goel, P. Gannala, W. D. S. Killgore, S. Jain, F. N. Jones-MacFarland, R. Khanna, A. Patwardhan, M. M. Ibrahim, Green light exposure improves pain and quality of life in fibromyalgia patients: A preliminary one-way crossover clinical trial. *Pain Med.* **22**, 118–130 (2021).
14. T. D. Lamb, Why rods and cones? *Eye (Lond.)* **30**, 179–185 (2016).
15. D. M. Berson, F. A. Dunn, M. Takao, Phototransduction by retinal ganglion cells that set the circadian clock. *Science* **295**, 1070–1073 (2002).
16. D. C. Fernandez, P. M. Fogerson, L. Lazzerini Ospri, M. B. Thomsen, R. M. Layne, D. Severin, J. Zhan, J. H. Singer, A. Kirkwood, H. Zhao, D. M. Berson, S. Hattar, Light affects mood and learning through distinct retina-brain pathways. *Cell* **175**, 71–84.e18 (2018).
17. K. An, H. Zhao, Y. Miao, Q. Xu, Y. F. Li, Y. Q. Ma, Y. M. Shi, J. W. Shen, J. J. Meng, Y. G. Yao, Z. Zhang, J. T. Chen, J. Bao, M. Zhang, T. Xue, A circadian rhythm-gated subcortical pathway for nighttime-light-induced depressive-like behaviors in mice. *Nat. Neurosci.* **23**, 869–880 (2020).
18. X. Huang, P. Huang, L. Huang, Z. Hu, X. Liu, J. Shen, Y. Xi, Y. Yang, Y. Fu, Q. Tao, S. Lin, A. Xu, F. Xu, T. Xue, K. F. So, H. Li, C. Ren, A visual circuit related to the nucleus reunions for the spatial-memory-promoting effects of light treatment. *Neuron* **109**, 347–362.e7 (2021).
19. L. Huang, Y. Xi, Y. Peng, Y. Yang, X. Huang, Y. Fu, Q. Tao, J. Xiao, T. Yuan, K. An, H. Zhao, M. Pu, F. Xu, T. Xue, M. Luo, K. F. So, C. Ren, A visual circuit related to habenula underlies the antidepressive effects of light therapy. *Neuron* **102**, 128–142.e8 (2019).
20. Z. Hu, Y. Mu, L. Huang, Y. Hu, Z. Chen, Y. Yang, X. Huang, Y. Fu, Y. Xi, S. Lin, Q. Tao, F. Xu, K. F. So, C. Ren, A visual circuit related to the periaqueductal gray area for the antinociceptive effects of bright light treatment. *Neuron* **110**, 1712–1727.e7 (2022).
21. D. Yates, Shining a light on pain. *Nat. Rev. Neurosci.* **23**, 253 (2022).
22. R. Nosedá, C. A. Bernstein, R. R. Nir, A. J. Lee, A. B. Fulton, S. M. Bertisch, A. Hovaguimian, D. M. Cestari, R. Saavedra-Walker, D. Borsook, B. L. Doran, C. Buettner, R. Burstein, Migraine photophobia originating in cone-driven retinal pathways. *Brain* **139**, 1971–1986 (2016).
23. C. A. Bernstein, R. R. Nir, R. Nosedá, A. B. Fulton, S. Huntington, A. J. Lee, S. M. Bertisch, A. Hovaguimian, C. Buettner, D. Borsook, R. Burstein, The migraine eye: Distinct rod-driven retinal pathways' response to dim light challenges the visual cortex hyperexcitability theory. *Pain* **160**, 569–578 (2019).

24. A. Monavarfeshani, U. Sabbagh, M. A. Fox, Not a one-trick pony: Diverse connectivity and functions of the rodent lateral geniculate complex. *Vis. Neurosci.* **34**, E012 (2017).
25. A. Pienaar, L. Walmsley, E. Hayter, M. Howarth, T. M. Brown, Commissural communication allows mouse intergeniculate leaflet and ventral lateral geniculate neurons to encode interocular differences in irradiance. *J. Physiol.* **596**, 5461–5481 (2018).
26. U. Sabbagh, G. Govindaiah, R. D. Somaiya, R. V. Ha, J. C. Wei, W. Guido, M. A. Fox, Diverse GABAergic neurons organize into subtype-specific sublaminae in the ventral lateral geniculate nucleus. *J. Neurochem.* **159**, 479–497 (2021).
27. A. Francois, S. A. Low, E. I. Sypek, A. J. Christensen, C. Sotoudeh, K. T. Beier, C. Ramakrishnan, K. D. Ritola, R. Sharif-Naeini, K. Deisseroth, S. L. Delp, R. C. Malenka, L. Luo, A. W. Hantman, G. Scherrer, A brainstem-spinal cord inhibitory circuit for mechanical pain modulation by GABA and enkephalins. *Neuron* **93**, 822–839.e6 (2017).
28. G. Corder, D. C. Castro, M. R. Bruchas, G. Scherrer, Endogenous and exogenous opioids in pain. *Annu. Rev. Neurosci.* **41**, 453–473 (2018).
29. S. Nagar, V. Krishnamoorthy, P. Cherukuri, V. Jain, N. K. Dhinra, Early remodeling in an inducible animal model of retinal degeneration. *Neuroscience* **160**, 517–529 (2009).
30. E. Soucy, Y. S. Wang, S. Nirenberg, J. Nathans, M. Meister, A novel signaling pathway from rod photoreceptors to ganglion cells in mammalian retina. *Neuron* **21**, 481–493 (1998).
31. H. Park, S. B. Jabbar, C. C. Tan, C. S. Sidhu, J. Abey, F. Aseem, G. Schmid, P. M. Iuvone, M. T. Pardue, Visually-driven ocular growth in mice requires functional rod photoreceptors. *Invest. Ophthalmol. Vis. Sci.* **55**, 6272–6279 (2014).
32. D. Goz, K. Studholme, D. A. Lappi, M. D. Rollag, I. Provencio, L. P. Morin, Targeted destruction of photosensitive retinal ganglion cells with a saporin conjugate alters the effects of light on mouse circadian rhythms. *PLOS ONE* **3**, e3153 (2008).
33. A. J. Emanuel, M. T. Do, Melanopsin tristability for sustained and broadband phototransduction. *Neuron* **85**, 1043–1055 (2015).
34. B. Zingg, X. L. Chou, Z. G. Zhang, L. Mesik, F. Liang, H. W. Tao, L. I. Zhang, AAV-mediated anterograde transsynaptic tagging: Mapping corticocollicular input-defined neural pathways for defense behaviors. *Neuron* **93**, 33–47 (2017).
35. Y. Diao, L. Cui, Y. Chen, T. J. Burbridge, W. Han, B. Wirth, N. Sestan, M. C. Crair, J. Zhang, Reciprocal connections between cortex and thalamus contribute to retinal axon targeting to dorsal lateral geniculate nucleus. *Cereb. Cortex* **28**, 1168–1182 (2018).
36. J. M. Roberts, H. Ennajdaoui, C. Edmondson, B. Wirth, J. R. Sanford, B. Chen, Splicing factor TRA2B is required for neural progenitor survival. *J. Comp. Neurol.* **522**, 372–392 (2014).
37. T. Sonoda, J. Y. Li, N. W. Hayes, J. C. Chan, Y. Okabe, S. Belin, H. Nawabi, T. M. Schmidt, A noncanonical inhibitory circuit dampens behavioral sensitivity to light. *Science* **368**, 527–531 (2020).
38. J. Hannibal, P. Hindersson, J. Ostergaard, B. Georg, S. Heegaard, P. J. Larsen, J. Fahrenkrug, Melanopsin is expressed in PACAP-containing retinal ganglion cells of the human retino-hypothalamic tract. *Invest. Ophthalmol. Vis. Sci.* **45**, 4202–4209 (2004).
39. P. G. Finlayson, R. Iezzi, Glutamate stimulation of retinal ganglion cells in normal and s334ter-4 rat retinas: A candidate for a neurotransmitter-based retinal prosthesis. *Invest. Ophthalmol. Vis. Sci.* **51**, 3619–3628 (2010).
40. R. A. Pinol, R. Bateman, D. Mendelowitz, Optogenetic approaches to characterize the long-range synaptic pathways from the hypothalamus to brain stem autonomic nuclei. *J. Neurosci. Methods* **210**, 238–246 (2012).
41. L. Petreanu, T. Mao, S. M. Sternson, K. Svoboda, The subcellular organization of neocortical excitatory connections. *Nature* **457**, 1142–1145 (2009).
42. B. R. Rost, J. Wietek, O. Yizhar, D. Schmitz, Optogenetics at the presynapse. *Nat. Neurosci.* **25**, 984–998 (2022).
43. M. E. Harrington, The ventral lateral geniculate nucleus and the intergeniculate leaflet: Interrelated structures in the visual and circadian systems. *Neurosci. Biobehav. Rev.* **21**, 705–727 (1997).
44. Z. Zhang, Y. Li, X. Lv, L. Zhao, X. Wang, VLM catecholaminergic neurons control tumor growth by regulating CD8<sup>+</sup> T cells. *Proc. Natl. Acad. Sci. U.S.A.* **118**, e2103505118 (2021).
45. R. Y. Moore, R. Weis, M. M. Moga, Efferent projections of the intergeniculate leaflet and the ventral lateral geniculate nucleus in the rat. *J. Comp. Neurol.* **420**, 398–418 (2000).
46. J. A. Stamford, Descending control of pain. *Br. J. Anaesth.* **75**, 217–227 (1995).
47. K. Cheng, L. F. Martin, M. J. Slepian, A. M. Patwardhan, M. M. Ibrahim, Mechanisms and pathways of pain photobiomodulation: A narrative review. *J. Pain* **22**, 763–777 (2021).
48. G. Balbinot, C. P. Schuch, P. S. D. Nascimento, F. J. Lanferdini, M. Casanova, B. M. Baroni, M. A. Vaz, Photobiomodulation therapy partially restores cartilage integrity and reduces chronic pain behavior in a rat model of osteoarthritis: Involvement of spinal glial modulation. *Cartilage* **13**, 13095–13215 (2019).
49. L. G. Langella, H. L. Casalechi, S. S. Tomazoni, D. S. Johnson, R. Albertini, R. C. Pallotta, R. L. Marcos, P. T. C. de Carvalho, E. C. P. Leal-Junior, Photobiomodulation therapy (PBMT) on acute pain and inflammation in patients who underwent total hip arthroplasty—A randomized, triple-blind, placebo-controlled clinical trial. *Lasers Med. Sci.* **33**, 1933–1940 (2018).
50. G. R. Pigatto, M. H. S. Quinteiro, R. L. Nunes-de-Souza, N. C. Coimbra, N. A. Parizotto, Low-intensity photobiomodulation decreases neuropathic pain in paw ischemia-reperfusion and spared nervus ischiadicus injury experimental models. *Pain Pract.* **20**, 371–386 (2020).
51. V. Leichtfried, R. Matteucci Gothe, W. Kantner-Rumplair, M. Mair-Raggautz, C. Bartenbach, H. Guggenbichler, D. Gehmacher, L. Jonas, M. Aigner, D. Winkler, W. Schobersberger, Short-term effects of bright light therapy in adults with chronic nonspecific back pain: A randomized controlled trial. *Pain Med.* **15**, 2003–2012 (2014).
52. M. Malter Cohen, D. Jing, R. R. Yang, N. Tottenham, F. S. Lee, B. J. Casey, Early-life stress has persistent effects on amygdala function and development in mice and humans. *Proc. Natl. Acad. Sci. U.S.A.* **110**, 18274–18278 (2013).
53. R. Nosedá, V. Kainz, M. Jakubowski, J. J. Gooley, C. B. Saper, K. Digre, R. Burstein, A neural mechanism for exacerbation of headache by light. *Nat. Neurosci.* **13**, 239–245 (2010).
54. D. Song, Y. Song, M. Hadziahmetovic, Y. Zhong, J. L. Dunaief, Systemic administration of the iron chelator deferiprone protects against light-induced photoreceptor degeneration in the mouse retina. *Free Radic. Biol. Med.* **53**, 64–71 (2012).
55. C. D. Charvet, A. Saadane, M. Wang, R. G. Salomon, H. Brunengraber, I. V. Turko, I. A. Pikuleva, Pretreatment with pyridoxamine mitigates isolevuglandin-associated retinal effects in mice exposed to bright light. *J. Biol. Chem.* **288**, 29267–29280 (2013).
56. C. Grimm, C. E. Reme, Light damage as a model of retinal degeneration. *Methods Mol. Biol.* **935**, 87–97 (2013).
57. M. Bian, Y. Zhang, X. Du, J. Xu, J. Cui, J. Gu, W. Zhu, T. Zhang, Y. Chen, Apigenin-7-digluconide protects retinas against bright light-induced photoreceptor degeneration through the inhibition of retinal oxidative stress and inflammation. *Brain Res.* **1663**, 141–150 (2017).
58. M. Bian, X. Du, J. Cui, P. Wang, W. Wang, W. Zhu, T. Zhang, Y. Chen, Celastrol protects mouse retinas from bright light-induced degeneration through inhibition of oxidative stress and inflammation. *J. Neuroinflammation* **13**, 50 (2016).
59. W. T. Keenan, A. C. Rupp, R. A. Ross, P. Somasundaram, S. Hiriyanna, Z. Wu, T. C. Badea, P. R. Robinson, B. B. Lowell, S. S. Hattar, A visual circuit uses complementary mechanisms to support transient and sustained pupil constriction. *eLife* **5**, e15392 (2016).
60. T. Breuninger, C. Puller, S. Haverkamp, T. Euler, Chromatic bipolar cell pathways in the mouse retina. *J. Neurosci.* **31**, 6504–6517 (2011).
61. D. J. Denman, J. A. Luviano, D. R. Ollerenshaw, S. Cross, D. Williams, M. A. Buice, S. R. Olsen, R. C. Reid, Mouse color and wavelength-specific luminance contrast sensitivity are non-uniform across visual space. *eLife* **7**, e31209 (2018).
62. W. B. Thoreson, D. M. Dacey, Diverse cell types, circuits, and mechanisms for color vision in the vertebrate retina. *Physiol. Rev.* **99**, 1527–1573 (2019).
63. M. Joesch, M. Meister, A neuronal circuit for colour vision based on rod-cone opponency. *Nature* **532**, 236–239 (2016).
64. K. P. Szatko, M. M. Korympidou, Y. Ran, P. Berens, D. Dalkara, T. Schubert, T. Euler, K. Franke, Neural circuits in the mouse retina support color vision in the upper visual field. *Nat. Commun.* **11**, 3481 (2020).
65. E. E. Benarroch, The melanopsin system: Phototransduction, projections, functions, and clinical implications. *Neurology* **76**, 1422–1427 (2011).
66. C. Beier, Z. Zhang, M. Yurgel, S. Hattar, Projections of ipRGCs and conventional RGCs to retinorecipient brain nuclei. *J. Comp. Neurol.* **529**, 1863–1875 (2021).
67. S. Hammer, G. L. Carrillo, G. Govindaiah, A. Monavarfeshani, J. S. Bircher, J. Su, W. Guido, M. A. Fox, Nuclei-specific differences in nerve terminal distribution, morphology, and development in mouse visual thalamus. *Neural Dev.* **9**, 16 (2014).
68. U. Sabbagh, A. Monavarfeshani, K. Su, M. Zabet-Moghadam, J. Cole, E. Carnival, J. Su, M. Mirzaei, V. Gupta, G. H. Salekdeh, M. A. Fox, Distribution and development of molecularly distinct perineuronal nets in visual thalamus. *J. Neurochem.* **147**, 626–646 (2018).
69. U. M. Ciftcioglu, V. Suresh, K. R. Ding, F. T. Sommer, J. A. Hirsch, Visual Information processing in the ventral division of the mouse lateral geniculate nucleus of the thalamus. *J. Neurosci.* **40**, 5019–5032 (2020).
70. J. W. Moulard, A. Pienaar, C. Williams, A. J. Watson, R. J. Lucas, T. M. Brown, Extensive cone-dependent spectral opponency within a discrete zone of the lateral geniculate nucleus supporting mouse color vision. *Curr. Biol.* **31**, 3391–3400.e4 (2021).
71. W. Yu, D. Pati, M. M. Pina, K. T. Schmidt, K. M. Boyt, A. C. Hunker, L. S. Zweifel, Z. A. McElligott, T. L. Kash, Periaqueductal gray/dorsal raphe dopamine neurons contribute to sex differences in pain-related behaviors. *Neuron* **109**, 1365–1380.e5 (2021).
72. I. Sora, M. Funada, G. R. Uhl, The  $\mu$ -opioid receptor is necessary for [d-Pen2,d-Pen5]enkephalin-induced analgesia. *Eur. J. Pharmacol.* **324**, R1–R2 (1997).
73. R. W. Hurley, D. L. Hammond, Contribution of endogenous enkephalins to the enhanced analgesic effects of supraspinal mu opioid receptor agonists after inflammatory injury. *J. Neurosci.* **21**, 2536–2545 (2001).
74. A. E. Kalyuzhny, M. W. Wessendorf, CNS GABA neurons express the mu-opioid receptor: Immunocytochemical studies. *Neuroreport* **8**, 3367–3372 (1997).



75. C. Li, J. A. Sugam, E. G. Lowery-Gionta, Z. A. McElligott, N. M. McCall, A. J. Lopez, J. M. McKlveen, K. E. Pleil, T. L. Kash, Mu opioid receptor modulation of dopamine neurons in the periaqueductal gray/dorsal raphe: A role in regulation of pain. *Neuropsychopharmacology* **41**, 2122–2132 (2016).
76. A. Mansour, C. A. Fox, S. Burke, F. Meng, R. C. Thompson, H. Akil, S. J. Watson, Mu, delta, and kappa opioid receptor mRNA expression in the rat CNS: An in situ hybridization study. *J. Comp. Neurol.* **350**, 412–438 (1994).
77. Y. Zhu, M.-S. Hsu, J. E. Pintar, Developmental expression of the  $\mu$ ,  $\kappa$ , and  $\delta$  opioid receptor mRNAs in mouse. *J. Neurosci.* **18**, 2538–2549 (1998).
78. T. M. Schmidt, N. M. Alam, S. Chen, P. Kofuji, W. Li, G. T. Prusky, S. Hattar, A role for melanopsin in alpha retinal ganglion cells and contrast detection. *Neuron* **82**, 781–788 (2014).
79. J. L. Ecker, O. N. Dumitrescu, K. Y. Wong, N. M. Alam, S. K. Chen, T. LeGates, J. M. Renna, G. T. Prusky, D. M. Berson, S. Hattar, Melanopsin-expressing retinal ganglion-cell photoreceptors: Cellular diversity and role in pattern vision. *Neuron* **67**, 49–60 (2010).
80. M. J. Millan, Descending control of pain. *Prog. Neurobiol.* **66**, 355–474 (2002).
81. A. Sandri, M. P. Cecchini, M. Riello, A. Zanini, R. Nocini, M. Fiorio, M. Tinazzi, Pain, smell, and taste in adults: A narrative review of multisensory perception and interaction. *Pain Ther.* **10**, 245–268 (2021).
82. M. Riello, M. P. Cecchini, A. Zanini, M. Di Chiappari, M. Tinazzi, M. Fiorio, Perception of phasic pain is modulated by smell and taste. *Eur. J. Pain* **23**, 1790–1800 (2019).
83. X. Xu, I. L. Hanganu-Opatz, M. Bieler, Cross-talk of low-level sensory and high-level cognitive processing: Development, mechanisms, and relevance for cross-modal abilities of the brain. *Front. Neurobot.* **14**, 7 (2020).
84. M. M. Hansen, R. Jones, K. Tocchini, Shinrin-Yoku (forest bathing) and nature therapy: A state-of-the-art review. *Int. J. Environ. Res. Public Health* **14**, 851 (2017).
85. S. Gil, L. Le Bigot, Seeing life through positive-tinted glasses: Color-meaning associations. *PLOS ONE* **9**, e104291 (2014).
86. A. Kanai, S. Matsumoto, N. Hayashi, J. Shimao, Y. Nagahara, Visual/emotional stimuli and treatment with antidepressants alter Numerical Rating Scale score in patients with chronic pain. *J. Clin. Anesth.* **36**, 90–93 (2017).
87. K. Wiercioch-Kuzianik, P. Babel, Color hurts. The effect of color on pain perception. *Pain Med.* **20**, 1955–1962 (2019).
88. D. M. Berson, A. M. Castrucci, I. Provencio, Morphology and mosaics of melanopsin-expressing retinal ganglion cell types in mice. *J. Comp. Neurol.* **518**, 2405–2422 (2010).
89. L. P. Muller, M. T. Do, K. W. Yau, S. He, W. H. Baldrige, Tracer coupling of intrinsically photosensitive retinal ganglion cells to amacrine cells in the mouse retina. *J. Comp. Neurol.* **518**, 4813–4824 (2010).
90. M. Hatori, H. Le, C. Vollmers, S. R. Keding, N. Tanaka, T. Buch, A. Waisman, C. Schmedt, T. Jegla, S. Panda, Inducible ablation of melanopsin-expressing retinal ganglion cells reveals their central role in non-image forming visual responses. *PLOS ONE* **3**, e2451 (2008).

**Acknowledgments:** We thank T. Xue (University of Science and Technology of China) for critical reading and suggestion on the manuscript. We thank H. Yang (Institute of Semiconductors, CAS) for providing the LED light cabinet and J. Zhang (Fudan University) for suggestions on central visual system experiments and giving some *Emx1*-Cre. We also thank S. Hattar (National Institute of Mental Health) for providing *Opn4*-Cre mice, T.-W. Huang (Shenzhen Institutes of Advanced Technology, CAS) for giving some *Penk*-Cre mice, B. Wirth (Institute of Human Genetics, Cologne) for providing *Tra2 $\beta$ <sup>flax/flax</sup>* mice, and T. Xue (University of Science and Technology of China) for giving *Opn4<sup>-/-</sup>* and *Opn4*-tdTomato mice. **Funding:** This work was supported by the National Key Research and Development Program of China (2021ZD0203205 and 2017YFB0403803 to Y.-Q.Z.; 2022ZD0208604 and 2022ZD0208605 to S.-J.W.), the National Natural Science Foundation of China (31930042 and 82130032 to Y.-Q.Z.; 81790640 and 82070993 to S.-J.W.), Shanghai Municipal Science and Technology Major Project grant 2018SHZDZX01 to Y.-Q.Z., and ZJLab and Shanghai Center for Brain Science and Brain-Inspired Technology (to Y.-Q.Z.). **Author contributions:** Y.-Q.Z. conceived the idea and supervised the project. Y.-Q.Z., S.-J.W., H.C., and Y.-L.T. designed the experiments. Y.-L.T. performed surgery, fluorescent ISH, real-time PCR, and fiber photometry experiments. Y.-L.T. and Z.-R.Z. performed behavioral and immunohistochemical experiments. A.-L.L. performed intravitreal injection, ERG recording, and immunohistochemical staining of retina. S.-S.L. performed slice recording experiments. H.C. performed some immunohistochemical experiments and participated in data discussion. Y.-Q.Z. and Y.-L.T. analyzed the data and prepared final figures. Y.-L.T., S.-J.W., and Y.-Q.Z. wrote the manuscript. **Competing interests:** The authors declare that they have no competing interests. **Data and materials availability:** All data associated with this study are present in the paper or the Supplementary Materials. *Tra2 $\beta$ <sup>flax/flax</sup>* mice are available from B. Wirth under a material transfer agreement with University of Cologne, and *Opn4<sup>-/-</sup>* and *Opn4*-tdTomato mice are available from Tian Xue under a material transfer agreement with University of Science and Technology of China.

Submitted 21 April 2022

Accepted 15 November 2022

Published 7 December 2022

10.1126/scitranslmed.abq6474

## Green light analgesia in mice is mediated by visual activation of enkephalinergic neurons in the ventrolateral geniculate nucleus

Yu-Long Tang Ai-Lin Liu Su-Su Lv Zi-Rui Zhou Hong Cao Shi-Jun Weng Yu-Qiu Zhang

*Sci. Transl. Med.*, 14 (674), eabq6474. • DOI: 10.1126/scitranslmed.abq6474

### View the article online

<https://www.science.org/doi/10.1126/scitranslmed.abq6474>

### Permissions

<https://www.science.org/help/reprints-and-permissions>

Use of this article is subject to the [Terms of service](#)